Volume 41
Number 5
May 2024
Pages 703–862

Natural Product Reports

rsc.li/npr

ISSN 0265-0568

ROYAL SOCIETY OF CHEMISTRY

REVIEW ARTICLE
Isabel Desgagné-Penix *et al.*
Unveiling Amaryllidaceae alkaloids: from biosynthesis to antiviral potential – a review

Natural Product Reports

ROYAL SOCIETY OF CHEMISTRY

REVIEW

View Article Online
View Journal | View Issue

Cite this: *Nat. Prod. Rep.*, 2024, **41**, 721

Unveiling Amaryllidaceae alkaloids: from biosynthesis to antiviral potential – a review

Thilina U. Jayawardena, †[a] Natacha Merindol, †[a] Nuwan Sameera Liyanage [a] and Isabel Desgagné-Penix *[ab]

Covering: 2017 to 2023 (now)

Amaryllidaceae alkaloids (AAs) are a unique class of specialized metabolites containing heterocyclic nitrogen bridging that play a distinct role in higher plants. Irrespective of their diverse structures, most AAs are biosynthesized *via* intramolecular oxidative coupling. The complex organization of biosynthetic pathways is constantly enlightened by new insights owing to the advancement of natural product chemistry, synthetic organic chemistry, biochemistry, systems and synthetic biology tools and applications. These promote novel compound identification, trace-level metabolite quantification, synthesis, and characterization of enzymes engaged in AA catalysis, enabling the recognition of biosynthetic pathways. A complete understanding of the pathway benefits biotechnological applications in the long run. This review emphasizes the structural diversity of the AA specialized metabolites involved in biogenesis although the process is not entirely defined yet. Moreover, this work underscores the pivotal role of synthetic and enantioselective studies in justifying biosynthetic conclusions. Their prospective candidacy as lead constituents for antiviral drug discovery has also been established. However, a complete understanding of the pathway requires further interdisciplinary efforts in which antiviral studies address the structure–activity relationship. This review presents current knowledge on the topic.

Received 26th September 2023

DOI: 10.1039/d3np00044c

rsc.li/npr

[a]*Department of Chemistry, Biochemistry, and Physics, Université du Québec à Trois-Rivières, Trois-Rivières, QC, G8Z 4M3, Canada. E-mail: Isabel.Desgagne-Penix@uqtr.ca*

[b]*Plant Biology Research Group, Université du Québec à Trois-Rivières, Trois-Rivières, QC, Canada*

† These authors contributed equally to this work.

1 Introduction

1.1 Alkaloids

Alkaloids are organic compounds containing basic nitrogen. Most alkaloids are derived from amino acids, such as phenylalanine, tyrosine, tryptophan, and lysine, and represent a wide range of chemical structures. Although most alkaloids are isolated from plants, they are found in microorganisms, marine organisms,[10,11] and, interestingly, terrestrial animals, such as insects.[12]

Alkaloids are often classified based on their carbon skeleton. Indole and isoquinoline alkaloids are the two leading groups in terms of number. Tropane, pyridine, pyrrolizidine, and steroidal alkaloids are also part of this large family.[15] Moreover, alkaloids are possibly categorized according to their botanical backgrounds, such as opium alkaloids, cactus alkaloids, *Solanum* alkaloids, and Amaryllidaceae alkaloids.[16]

Two tyrosine derivatives, dopamine and 4-hydroxyphenylacetaldehyde, condense and undergo cyclization to give rise to benzylisoquinoline alkaloid (BIA) precursor, (*S*)-norcoclaurine. The product undergoes a series of aromatic hydroxylation and methylation enzymatic reactions to reach (*S*)-reticuline. Most isoquinoline scaffolds dwell in (*S*)-reticuline as

Thilina U. Jayawardena

Thilina U. Jayawardena received his bachelor's in Chemistry from the University of Colombo. He earned a master's degree and PhD degree (2022) in Life Sciences, focusing on Natural Product Chemistry at Jeju National University under Prof. You-Jin Jeon. Currently, he is continuing his postdoctoral studies at the Université du Québec à Trois-Rivières (UQTR) under the mentorship of Prof. Isabel Desgagné-Penix, having previously served as a postdoctoral fellow at the University of Calgary. His research interests include natural product chemistry, medicinal chemistry, and bioactive molecules, with a particular emphasis on specialized metabolites.

Nuwan Sameera Liyanage

Nuwan Sameera Liyanage earned a bachelor's degree in plant science from the University of Colombo, Sri Lanka in 2013. He went on to complete his master's degree in ecology in 2020 from the Université du Québec en Abitibi-Témiscamingue. Currently, he is pursuing his PhD in Cellular and Molecular Biology at the Université du Québec à Trois-Rivières under the guidance of Prof. Isabel Desgagné-Penix. His doctoral research is focused on studying the N*-methyltransferases of Amaryllidaceae alkaloid biosynthesis.*

Natacha Merindol

Natacha Merindol obtained a PhD in microbiology and immunology from Université de Montréal in 2011. She conducted her first postdoctoral research at the INSERM Immunology unit in Lyon, working on inflammation and lymphoma and a second one at Université du Québec à Trois-Rivières (UQTR), specializing in virology. She now works as a research associate under Prof. Isabel Desgagné-Penix at UQTR, focusing on the discovery and characterization of the antiviral properties of Amaryllidaceae alkaloids and unraveling their biosynthesis. Her current projects incorporate several disciplines, such as virology, molecular biology, bioengineering, and molecular dynamics (photo credit: Isabelle Cardinal, UQTR).

Isabel Desgagné-Penix

Isabel Desgagné-Penix, a professor at the University of Québec at Trois-Rivières in Canada, has always been interested in the way plants make medicines. She holds a PhD in Cell and Molecular Biology (2008) from the University of Texas-San Antonio and has become a world pioneer in the use of advanced technologies for specialized plant metabolism research. She aims to elucidate the biosynthetic pathways of selected molecules and to develop alternative sources to produce them. Strongly involved in the promotion of women and indigenous people in science, she contributes, through her work, to designing and building new biological systems for purposes useful to humanity.

a common intermediate, leading to structural diversification. This main scaffold then undergoes functionalization reactions, such as *N*-, *O*-methylation, oxido-reduction, and oxidation bridge formation, resulting in the structural diversity of alkaloids.[17] BIA is more complex than simple isoquinoline alkaloids (benzene rings fused to the isoquinoline ring) because of their third aromatic ring. Many other alkaloid groups, such as protoberberines, protopines, pavines, and aporphines, are structurally related to BIA.

Due to its structure, alkaloid crystallization is not easy although its salt counterparts are crystallizable. The water solubility of alkaloids largely depends on the amine functional group, and this is readily protonated under acidic conditions. Despite having a conjugated double bond structure in most alkaloids, they appear to be colourless in most cases, and few highly conjugated structures are found to be coloured (*e.g.* sanguinarine and serpentine) and otherwise exhibit robust fluorescence (*e.g.* quinine). *N*-Oxidation leaves alkaloids vulnerable to stability. Further, heat, light, and solvents interfere with their stability. Higher stabilities of alkaloids are generally obtained in ethyl acetate, toluene, and alcoholic solutions.[18]

In this study, our aim is to investigate Amaryllidaceae alkaloids (AAs), giving priority to their structural diversity, metabolic pathway, and antiviral potential, which are discussed in detail in later sections.

1.2 Amaryllidaceae alkaloids

As the name implies, the special group of alkaloids is primarily observed in the Amaryllidaceae plant family *sensu* APG II.[19] Over 900 species clustered under 75 genera are distributed in multiple regions of the Amaryllidaceae plant family.[20] South Africa and South America cradle the major diversity, whereas the Mediterranean region has comparatively fewer genera. Habitats from seasonally dry rainforests to ephemeral pools provide locations for Amaryllidaceae plants to thrive. Current evidence supports the idea that the origin of the family lies in Africa.[21,22] The literature teaches of approximately 650 naturally occurring Amaryllidaceae alkaloids identified.[23,24] Amaryllidaceae plants are of ethnopharmacological value. They have been used in traditional medicine. Nair and Staden (2014) explained the extensive use of Amaryllidaceae (*Boophone disticha*) in traditional medicine by various indigenous populations, such as Sotho, Zhaso, Zulu, and San in South Africa.[25] Although not limited to Africa, the significant presence of Amaryllidaceae spans multiple ethnic groups worldwide. The ethnopharmacological relevance originates from its antifungal, antiparasitic, anti-inflammatory, insect antifeedant, and antibacterial effects. The deeper involvement of AAs as antibacterial agents is out of the scope of this review although a comprehensive review on the subject matter published by Nair *et al.* (2017) is worth referring to.[26]

The Amaryllidaceae family is unique because of its capability to produce structurally diverse alkaloids. Although their structure appears to be different, the formation of AA is known to occur *via* the intramolecular oxidative coupling of norbelladine. AAs are isoquinoline alkaloids, a well-conserved group in higher plants. However, biochemical and molecular phylogenetical studies suggest an evolutionary monophyletic role in basal angiosperms.[27] The group adopts the isoquinoline nucleus as the basic structural feature. The recent increase in the interest in isoquinoline alkaloids owing to their multimodal capacity has encouraged pharmacological research.[28,29] In evolutionary terms, isoquinoline alkaloids are presumed to play a role in an ancient conservative and survival strategy of defense mechanism. Further, isoquinoline alkaloids and phenylpropanoid derivatives (tannin and lignin) are proposed to have intrinsic biochemical and evolutive biosynthetic relationships explaining preferential biosynthesis and accumulation concepts.[30] Isoquinolines are again divided into subclasses from simple scaffolds to complex dimeric structures. The biosynthetic precursor for isoquinoline alkaloids is aromatic amino acid tyrosine. Three main groups of enzymes are involved in the process of generating AA: oxidoreductases, transferases, and lyases. Some of the oxidoreductases that catalyse the reactions are cytochromes P450 (CYP) and in most cases act in oxidative couplings and methylenedioxy bridge formation. Additionally, alkaloid biosynthesis requires stereo selective enzymes that lead to the formation of (*S*)-enantiomers.[30,31]

AA classification has been conducted using different methods by scientists according to their biogenesis, carbon skeleton and ring systems (Fig. 1). In the literature, a 9 ring-,[23,24] 12 ring-,[32] and 11 ring-[33] type classifications can be identified. However, these classifications over the years have been subjected to changes and modifications because of novel AA identified, similarities between groups and the non-specificities identified by each scientist. Therefore, it is difficult to establish a universal classification system because of its large scale and frequently updated databases of natural product chemistry research.

The identification of novel natural products and the elucidation of their biosynthetic and degradation pathways are essential for enhancing crop characteristics, advancing drug discovery, and driving innovation in synthetic biology. To make strides in identifying compounds and genes, it is crucial to map and annotate the metabolic landscape of plants comprehensively. Although contemporary technologies can readily accomplish the initial identification, the subsequent annotation and classification of metabolites remain a significant challenge that hinders rapid advancement. Untargeted metabolomics can detect the presence of a wide array of metabolites in plants without prior knowledge of their existence or identity. However, relying solely on factors such as mass-to-charge ratio (m/z), retention time, and ion abundance does not lead to unequivocal structural annotations of metabolites and does not provide evidence of their origin. This is because numerous metabolites share similar or even identical masses. These factors can introduce additional complexities in the interpretation of the results. A targeted approach involves determining the precursor of origin for metabolites through labelling. In this method, plant tissue is exposed to a metabolite that contains a radio/heavy isotope on one or more of its atoms. When stable isotope labelling, such as ^{13}C, is combined with mass

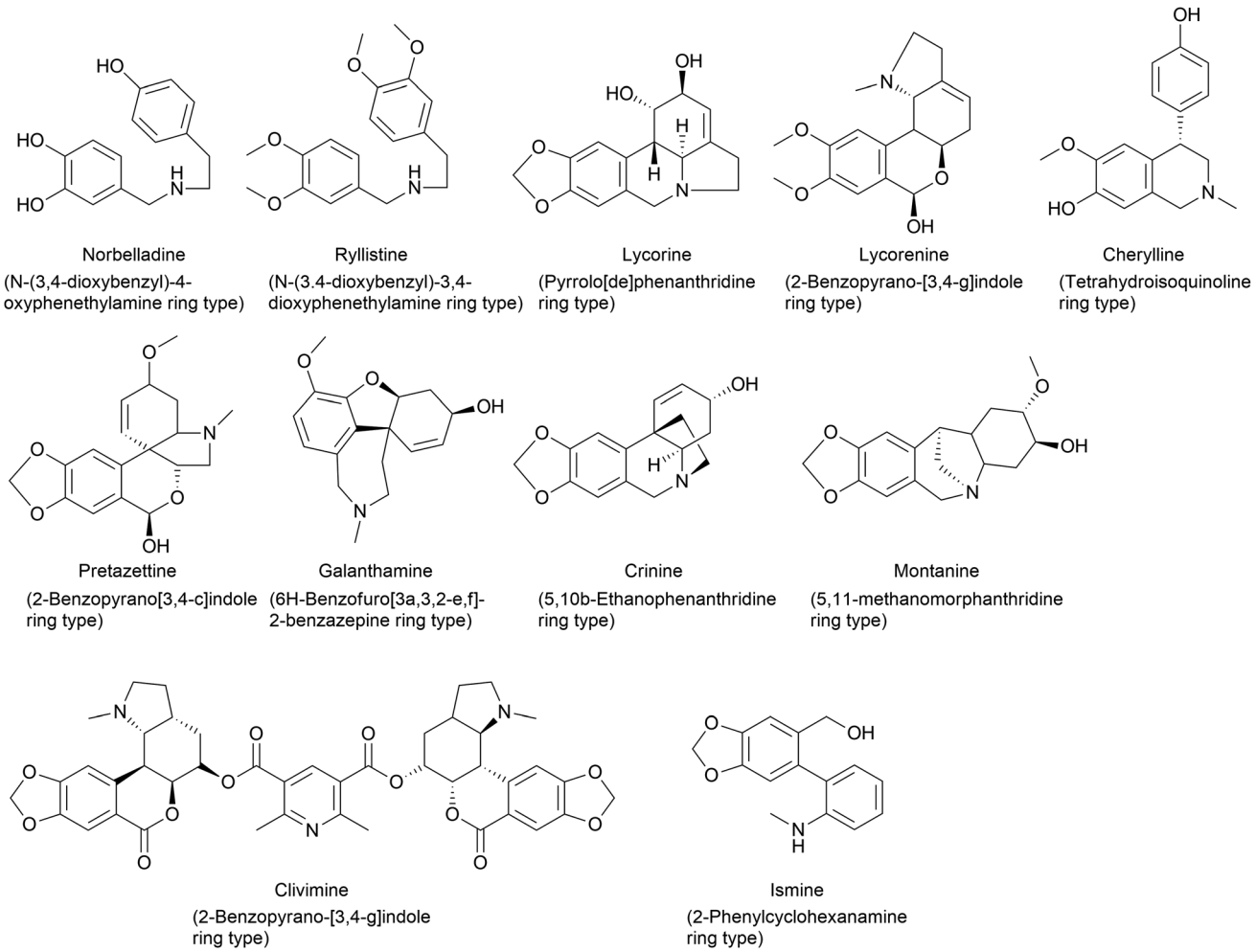

Fig. 1 Chemical structures representing ring type(s) present in Amaryllidaceae alkaloids depending on the carbon skeleton and the ring system.

spectrometry detection, it becomes possible to identify labelled metabolites and clarify their origin. The biochemical exploration of Amaryllidaceae alkaloid biosynthesis involves the use of labelled precursors and intermediates, leading to the formulation of biochemical models to produce different types of alkaloids. The ideas were initiated and implemented in the 1950s and 60s with radiolabelling.[34] Labelling experiments provide insights into the intermediates and reaction mechanisms of biosynthetic pathways, shedding light on their interactions and interrelationships.

2 Structural diversity and biogenesis of Amaryllidaceae alkaloids

2.1 Cherylline type

Cherylline is a 4-aryltetrahydroisoquinoline alkaloid isolated from Amaryllidaceae plants. The first attempt to isolate unknowingly cherylline-type alkaloid was conducted by Boit in 1954,[35] which was first named crinine. Its structure was later elucidated by Brossi and his team in 1970 (ref. 36) who named it cherylline. However, this was a racemic mixture of (+) and (−) isomers (given its C4 chiral center).[37,38] Comparatively, Schwartz and Scott took a different approach to the total synthesis of racemic cherylline using a biogenetically patterned pathway.[39] They yielded a quinone methide to achieve (±)-cherylline. Accordingly, in the synthetic literature, it is probable to predict that norbelladine moves to hydroxy-*O*,*N*-dimethylnorbelladine before forming the quinone methide. However, it is questionable whether methylation takes priority over hydroxylation. Despite the lack of previous records on the biosynthesis of cherylline, it has received much attention with regard to synthetic chemistry aspects and natural product isolation, even until today.[40–42]

Few studies regarding cherylline have been published since 2017. Shi *et al.* (2018) examined the one-pot synthesis of two constitutional isomers: (±)-latifine and (±)-cherylline.[40] Nair *et al.* (2020) reported the identification of cherylline and ambelline from the larvae of the *Crinum moorei* moth *Brithys crini*.[43] Ambelline is a crinane alkaloid and is discussed in a different subsection. Although isoquinoline alkaloids notoriously exhibit cytotoxicity, this study identified the alkaloids in plant leaves, moth larvae, and larvae excrement material by performing HPLC and LC-MS analysis, which was further confirmed by HRMS and NMR techniques. This study lacks the

tools that insects use to overcome the toxic effects of these compounds and opens up opportunities for prospective studies. Cherylline-type AA, cherylline, gigantelline, and gigantellinine were isolated from *Crinum jagus*.[42] According to the report, cherylline derivatives were isolated and identified for the first time in a given species. Both gigantelline and gigantellinine are predicted to emerge from cherylline given their common structural features. In the case of gigantellinine, the *para* substituted phenol group is modified by methylation to phenyl-OH and hydroxylation at the neighbouring *ortho* position, whereas in gigantelline, the C7 hydroxyl group is methylated. Gigantelline was unable to inhibit the activity of acetylcholinesterase (AChE) in a dose-dependent manner, whereas cherylline and gigantellinine showed positive outcomes. Furthermore, cherylline showed weak cytotoxic effects against the breast cancer cell line MCF-7. The study further established that purified cherylline and gigantellinine had an *S* configuration, while gigantelline was assigned to the *R* configuration. However, none of the recent studies have attempted any metabolic pathway evaluation. According to our understanding, cherylline could originate through the common precursor norbelladine *via* the proposed route depicted in Fig. 2.

2.2 Norbelladine/belladine-type

Norbelladine/belladine-type is the originating structure of alkaloids that leads to other types of AA, such as galanthamine, lycorine, and crinine *via* oxidative coupling. Phenylalanine is a precursor of protocatechuic aldehyde/3,4-dihydroxybenzaldehyde (3,4-DHBA) and combines with tyramine, which is yielded from tyrosine to produce the Shiff base (norcraugsodine).[44] Norbelladine/benzyl-1-phenylethylamine is formed by the reduction of the above, and subsequent methylation generates *O*-methylnorbelladine (Fig. 3).

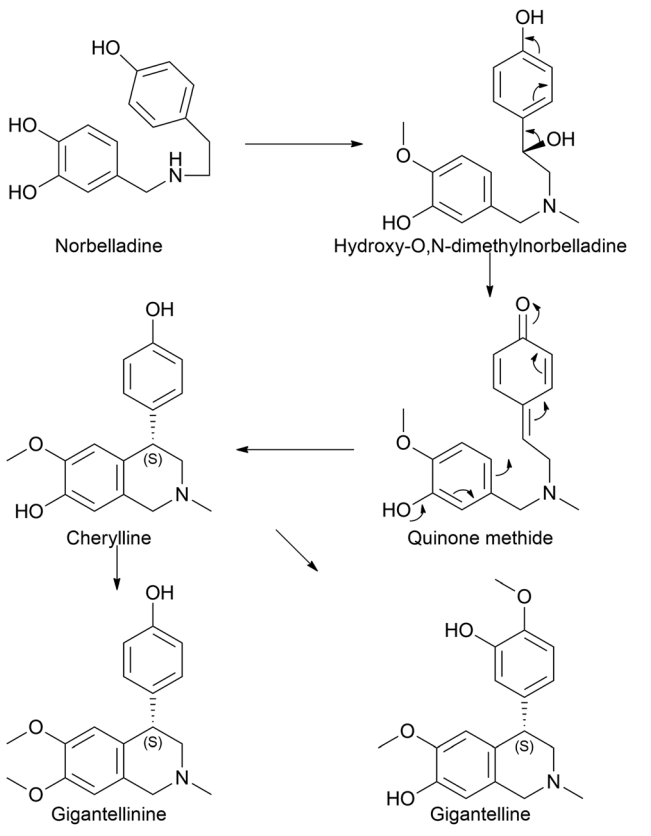

Fig. 2 Biosynthetic pathway of cherylline-type Amaryllidaceae alkaloids.

2.2.1 Norcraugsodine reductase and norbelladine synthase. Considering the chemistry (nucleophilic attack of tyramine, amine group on the protocatechuic aldehyde) associated with norcraugsodine formation, the condensation reaction occurs either non-enzymatically or within the active site of the reduction enzyme. The Schiff base previously described has also received attention in the pathway. Intermediate norcraugsodine lacks any methylation at the C6–C1 unit phenyl groups. In contrast, isocraugsodine is 4′-*O*-methylated, and craugsodine is 3′-*O*-methylated.[45] It is questionable whether norcraugsodine undergoes methylation to produce craugsodine and isocraugsodine or protocatechuic aldehyde analogues, such as vanillin and isovanillin, help derive these compounds through the Schiff base in the Mannich reaction. Isocraugsodine and its isomerism have been reported in *Crinum asiaticum*.[46] Kilgore and colleagues (2016) proposed a reaction mechanism for the reduction of norcraugsodine through the catalysis of noroxomaritidine reductase (NR), a short-chain alcohol dehydrogenase/reductase (SDR).[47] The research investigated the combination of tyramine with isovanillin, vanillin and piperonal analogues of 3,4-dihydroxybenzaldehyde, which yielded 4′-*O*-methylnorbelladine, 3′-*O*-methylnorbelladine, and 4-(2-((1,3-benzodioxol-5-ylmethyl)amino)ethyl) phenol, respectively. However, the NR-catalysed reaction of isovanillin and tyramine was 4-fold lower than that of 3,4-dihydroxybenzaldehyde. Further, NR could reduce an imine in the conversion of norcraugsodine to norbelladine, but the specific activity was lower than that of noroxomaritidine to oxomaritinamine, indicating a potential non-specific reaction. *In silico* docking studies demonstrated that the NR active site Tyr^{175} to be positioned near the imine group and NADPH. Lys^{179} interaction with Tyr^{175} leads to the polarization of the latter, allowing the OH group to assist the hydride transfer from NADPH to yield norbelladine.

Singh *et al.* (2018) argued that considering the first committed step in BIA formation *via* the condensation of dopamine and 4-hydroxyphenylacetaldehyde to form norcoclaurine, the same could be applied to norbelladine formation *via* the norcoclaurine synthase (NCS) ortholog in Amaryllidaceae identified as norbelladine synthase from *Narcissus pseudonarcissus* (*Np*NBS).[48] NCS and NBS are members of the same protein family, Bet v1/PR10. This can be classified into two groups: intracellular pathogenesis-related proteins (IPR) and (*S*)-norcoclaurine synthases (NCS). IPR proteins indicate cytosolic localization of NCS in subcellular compartments other than the cytosol considering its putative N-terminal signal peptides.[49] It was previously reported that this family, specifically the NCS group, played a pivotal role in alkaloid production.[50] The very same was discussed above in the presence of NR though in lower specific activity. The study left the question of whether tyramine and 3,4-DHBA were converted to norbelladine

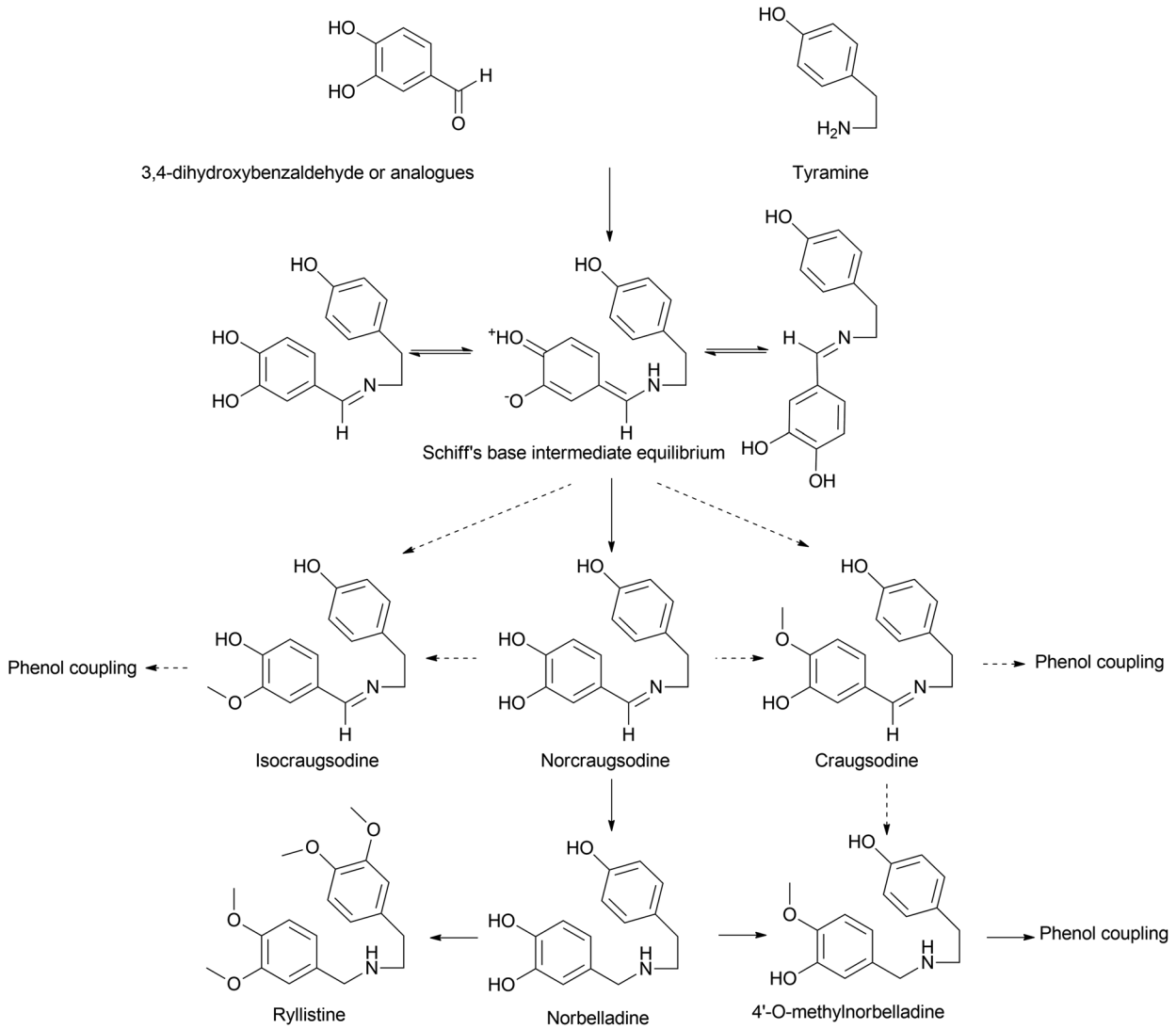

Fig. 3 Biosynthetic pathway of belladine-type Amaryllidaceae alkaloids. Interconversion of R1 and R2 in the C6–C1 unit may yield various components, including 3,4-DHBA, vanillin, isovanillin, and corresponding Schiff base intermediates. A dashed arrow represents potential outcomes.

via a single-step process under the catalysis of NBS or a two-step mechanism, as explained by Kilgore *et al.* (2014), involving NR.[51] However, further studies by our group[44] suggest that NBS and NR could cooperatively catalyze the reaction swiftly yet effectively through condensation and imine reduction to achieve norbelladine, avoiding the degradation of unstable norcraugsodine. A report on the NBS of *Leucojum aestivum* (*La*NBS) indicates recent elucidation of the enzyme at the molecular level with data on subcellular localization (likely cytosolic), suggesting that AA biosynthesis is initiated in the cytosol.[52] Phylogenetic analysis indicated that *La*NBS shares a high amino acid identity with *Np*NBS1 and *Np*NBS2. The catalytic activity of *La*NBS was confirmed *via* LC-MS/MS analysis, providing tyramine and 3,4-DHBA as substrates to produce norbelladine.

2.2.2 Norbelladine *O*-methyltransferase. The immediate next step is the conversion of norbelladine to 4′-*O*-methylnorbelladine to proceed to the belladine pathway as well as to other alkaloid ring types. The case was studied by Kilgore *et al.* (2014) for the first time by identifying the AA biosynthetic gene *N4OMT*, a methyltransferase specific to the 4′-*O*-position (*Np*N4*O*MT; *Narcissus* sp. *aff*. *Pseudonarcissus*).[51] However, a question was raised as to whether the preference would be given to methylate the *N*- or *O*-position, as well as the *O*-position. Similar K_m and k_{cat} values were observed for *N*-methylnorbelladine and norbelladine, indicating that there would be no preference for *N*-methylation. Among the multiple substrates tested, 3,4-DHBA had no product, suggesting that no methylation was possible before norbelladine formation. Similarly, its analogous components and counterpart to the formation of norbelladine did not yield any product, confirming the above proposition in their study. Interestingly, N4*O*MT can methylate dopamine, given its structural similarity to the methylated moiety, according to the authors. However, in this review, we question whether the methylated moiety is

structurally similar to protocatechuic aldehyde and not tyramine or its analogues.

A considerable increase in publications has been reported on other Amaryllidaceae *O*MTs related to norbelladine. Sun *et al.* (2018) characterized an *O*MT from *Lycoris aurea* (*La*OMT$_1$)[53] with activity on both caffeic acid and 3,4-DHBA towards both *meta* and *para* positions albeit with significant preferred methylation of the *meta* position. Similarly, this enzyme converted norbelladine into its successor 4′-*O*-methylnorbelladine but also into 3′-*O*-methylnorbelladine. Unlike *Np*N4*O*MT, *La*OMT$_1$ could convert caffeic acid to ferulic and isoferulic acids in the presence of methyl group donor *S*-adenosyl-L-methionine (SAM), and 3,4-DHBA yielded vanillin and isovanillin. However, 3,4-DHBA analogues, vanillin and isovanillin, were not methylated by *La*OMT$_1$ under their experimental conditions. This implies that once methylated, further methylation/double methylation was not a character at disposal with *La*OMT$_1$. The research further revealed that the enzyme was mainly localized in the cytoplasm and endosome.

Li *et al.* (2019) investigated *Lycoris radiata* *O*MT (*Lr*OMT).[54] They proposed that given the methoxy positions of different AAs, *O*-methylation involves different *O*MTs or a single *O*MT expressing multiple *O*-methylation activities. However, after successful molecular cloning, heterologous overexpression and functional characterization of *Lr*OMT, they report it to exhibit both *para*- and *meta*-*O*-methylation using norbelladine as substrate to produce 4′- and 3′-*O*-methylnorbelladine although moderate preferences towards *para*-OH, respectively. Comparatively, *La*OMT$_1$ previously reported by Sun *et al.*[53] (2018) preferred the *meta* position against its native substrate, caffeic acid. All three substrates, norbelladine, 3,4-DHBA, and caffeic acid, produced respective outputs with *Lr*OMT, demonstrating its promiscuity. At least two vicinal hydroxyl groups in the aromatic substrate analogue can be recognised by *O*MT. Catalysis of *O*-methylation by *Lr*OMT depended on the properties of the binding groups, *i.e.* electron donating amine groups (norbelladine, dopamine, 3,4-dihydroxybenzylamine, higenamine, (−)-epinephrine, (−)-norepinephrine, and 1,2,3,4-4*H*-6,7-isoquinolinediol) prefer *para* position, where electron withdrawing groups, such as carboxyl (caffeic acid) and aldehydes (3,4-DHBA, 5-hydroxyvanillin, 3,4,5-trihydroxybenzaldehyde, and ethyl 3,4-dihydroxybenzoate) (Fig. 4), favoured *meta* substitution. This summarized the difference of *Lr*OMT from *La*OMT$_1$ (ref. 53) and *Np*N4OMT.[51] This article further discusses the vitality of divalent cations in the reaction mixture. Magnesium (divalent, Mg^{2+}) was shown to increase the *O*-methylation potential, whereas Zn^{2+}, Cu^{2+} and EDTA (a divalent metal ion chelator) expressed significant inhibition. A recent study by Li *et al.* (2020) revealed *Lycoris longituba* *O*MT (*Ll*OMT) to be a class 1 *O*MT, where it catalyses norbelladine to generate 4′-*O*-methylnorbelladine.[55] However, they did not report any preferential methyl transfer by *Ll*OMT; in addition, their focus was more on

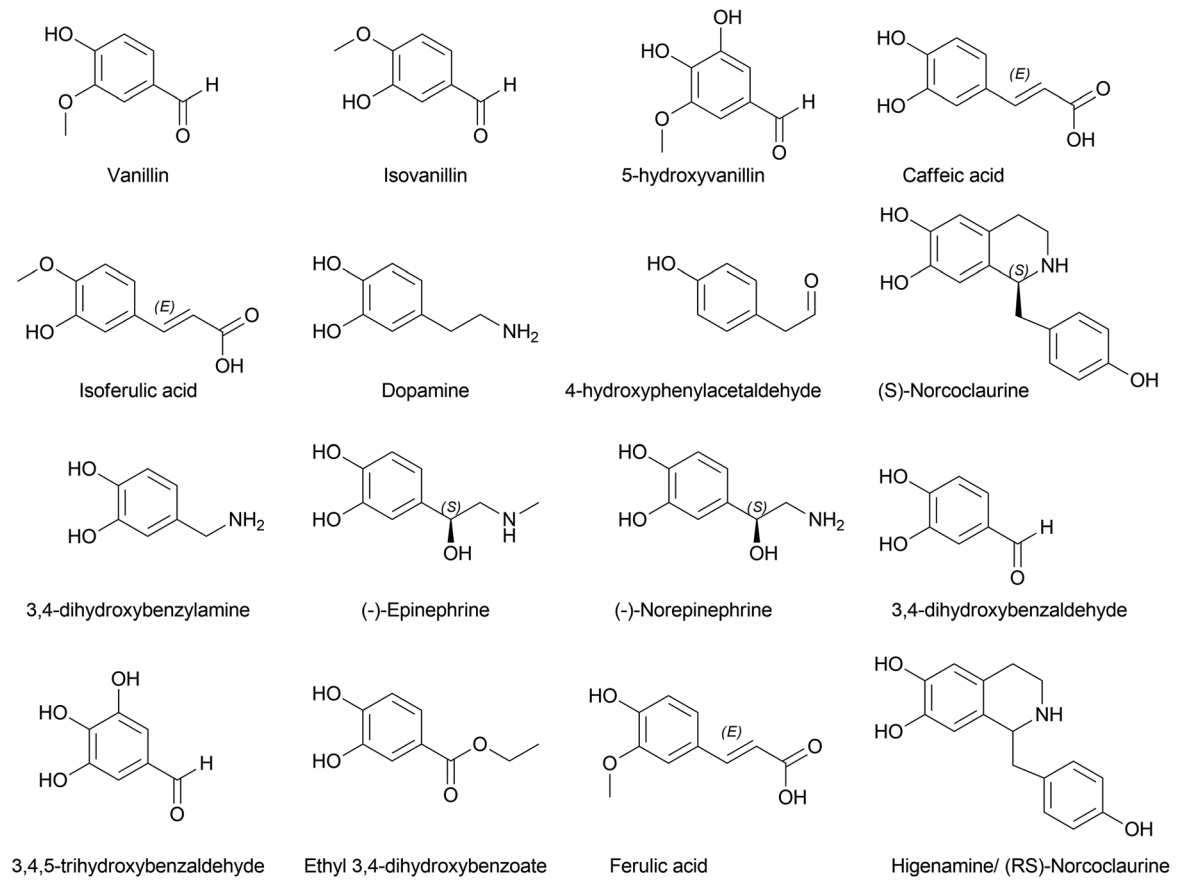

Fig. 4 Representative structures discussed in the norbelladine/belladine-type alkaloid formation.

the action of this particular enzyme on the expression of galanthamine content. Another report by the same team suggested that methyl jasmonate treatment on *L. longituba* induces the expression of NBS and 4′-*O*-methyltransferase.[56] *Narcissus* sp. in AA biosynthesis with respect to its putative genes based on galanthamine was assessed by Aleya (2021).[57] The study indicates the expression level of *Np*N4*O*MT variation between the field-grown bulb and basal tissues (significantly higher) compared to *in vitro* cultures (bulblet and callus). Differential expression of *Np*N4*O*MT leads to alkaloid biosynthesis in later steps and thus to cellular differentiation.

The belladine-type alkaloids can be extended to ryllistine, a 4-oxygenated norbelladine. Ghosal *et al.* (1984) specially mentioned this compound as a potential candidate for 1,2-epoxy-5,10*b*-ethanophenanthridine alkaloids, such as (−)crinine and powelline-type alkaloid synthesis, instead of reaching them *via* the oxidation of (−)oxocrinine owing to its co-occurrence with 1,2-β-epoxyalkaloids.[58] However, pathways reaching these compounds or their metabolism have been reported scarcely.

2.3 Downstream pathways: phenol coupling of 4′-*O*-methylnorbelladine

The plant kingdom possesses C–O or C–C phenol-couple reactions utilized in specialized metabolism processes, such as alkaloid, lignan, and lignin biosynthesis.[59] The reactions are highly regio- and/or stereo-selective often owing to cytochrome P450 (CYP) enzymes. A 1% of total gene annotations is estimated to be covered by CYPs in plant genomes, implying their key role in versatile reactions.[60] CYP is a diverse class of enzymes with multiple functions, including hydroxylation, oxide bridge formation, demethylation, carbon bond cleavage, skeleton rearrangements, and phenol coupling.[61] A detailed report on CYP in plant-specialized metabolism elaborating on unusual reactions was published by Mizutani and Sato (2011).[61] Multiple reports in the literature record its potential in salutaridine (CYP719A1), cyclodopeptide cyclo(1-Tyr-1-Tyr) (CYP121), and (*S*)-corytuberine (CYP80G2) biosynthesis, indicating CYP involvement in alkaloids.[59,62,63] Internal phenol coupling is reported here given its highly efficient and selective process. Distinct types of phenol coupling reactions are believed to occur owing to the proximity of the phenolic groups in precursor molecules, allowing for the formation of multiple products from a single substrate. This increases the diversity of alkaloids produced by the plant, which may provide a survival advantage. Alternatively, distinct coupling could occur within a single enzyme, CYP96, which may increase the efficiency of the reaction. CYP96 has evolved to catalyze specific types of coupling. Additionally, internal phenol coupling can avoid the need for the substrate to cross cell membranes and interact with other enzymes and molecules. This reduces the chances of substrate loss or competing reactions, which can increase the yield of the desired product.

Phenol coupling occurs in the late–late pathway of AA biosynthesis. Highly complex structures are formed owing to sequential phenolic coupling and reduction reactions. The pathway is characterised by the formation of a C–C bond between two phenolic precursors, leading to a new carbon skeleton. The common precursor 4′-*O*-methylnorbelladine is modified by the catalysis of CYP96 in Amaryllidaceae. For the first time, Barton and Cohen (1957)[64] proposed the oxidative coupling of Amaryllidaceae based on norbelladine or related compounds.[61] The condition suggested was the suitable protection of ring A phenolic group(s) *via* methylation. Oxidative coupling leads to distinct skeletons of AA. Secondary cyclization occurs *via* the oxidative coupling of *O*-methylnorbelladine, leading to restructuring and diversification. Three distinct pathways are suggested depending on the C–C bridge formation between ring A (C6–C1 unit) and C (C6–C2 unit): *para–ortho′*, *ortho–para′*, and *para–para′* (Fig. 5). Hydrogen abstraction from phenol believed to be an action initiated by the CYP leads to the delocalization of unpaired/radical electrons *via* resonance structure formation, and phenol radicals are then quenched by coupling, producing the aforementioned combinations. Multiple intermediates are formed in this process, determining the end product. Biosynthesis reactions conducted using radioisotope labels have contributed much to the understanding of the mechanisms and pathways in this step of AA biosynthesis.[65–68] A hypothetical pathway involving intermediates is presented in Fig. 5.

2.3.1 *Para–ortho′* phenol coupling: galanthamine and other dibenzofuran nucleus molecules. The *para–ortho′* coupling leads to the renowned compound galanthamine, holding a dibenzofuran nucleus. Eichhorn *et al.* (1998) suggest that 4′-*O*-methylnorbelladine produces a dienone and that a spontaneous closure of the ether bridge yields *N*-demethylnarwedine (nornarwedine) (Fig. 5 and 6).[65] The product has 2 stereocenters, leaving the choice of stereoselective reduction to produce norgalanthamine. Alternatively, the process could be initiated from *N*,*O*-dimethylnorbelladine instead of *O*-methylnorbelladine. The mechanism was studied using King Alfred daffodils *via* the integration of various dihydric phenols and (±)-[2-^{14}C] tyrosine. Successful incorporation of the precursor into galanthamine was observed with *N*,*O*-dimethylnorbelladine, *N*-methylnorbelladine, and norbelladine treatment but not with *O*-methylnorbelladine. Thus, this suggests that the order of conversion could be norbelladine to *N*-methylnorbelladine, to *N*,*O*-dimethylnorbelladine, and ultimately to galanthamine (Fig. 6).[69] If this pathway occurs, there would be no direct nornarwedine formation, and nornarwedine-to-narwedine must be explained *via* another mechanism. Concerning the similarities in the structures of galanthamine and narwedine, they may remain in equilibrium through oxidoreductase. Further, narwedine is not a direct precursor of galanthamine according to Eichhorn *et al.* (1998), with ^{13}C labelled 4′-*O*-methylnorbelladine treatment in *L. aestivum*.[65] However, there is no recent report on the pathway analysis of galanthamine synthesis through *C–C* coupling other than the minute amount because of a by-product in the study conducted by Kilgore *et al.* (2016).[70] Lycoramine first isolated and characterized from *L. radiata* serves another interesting aspect of pathway.[71] The catalytic hydrogenation of galanthamine readily reduced its double bond, resulting in lycoramine. A conclusive

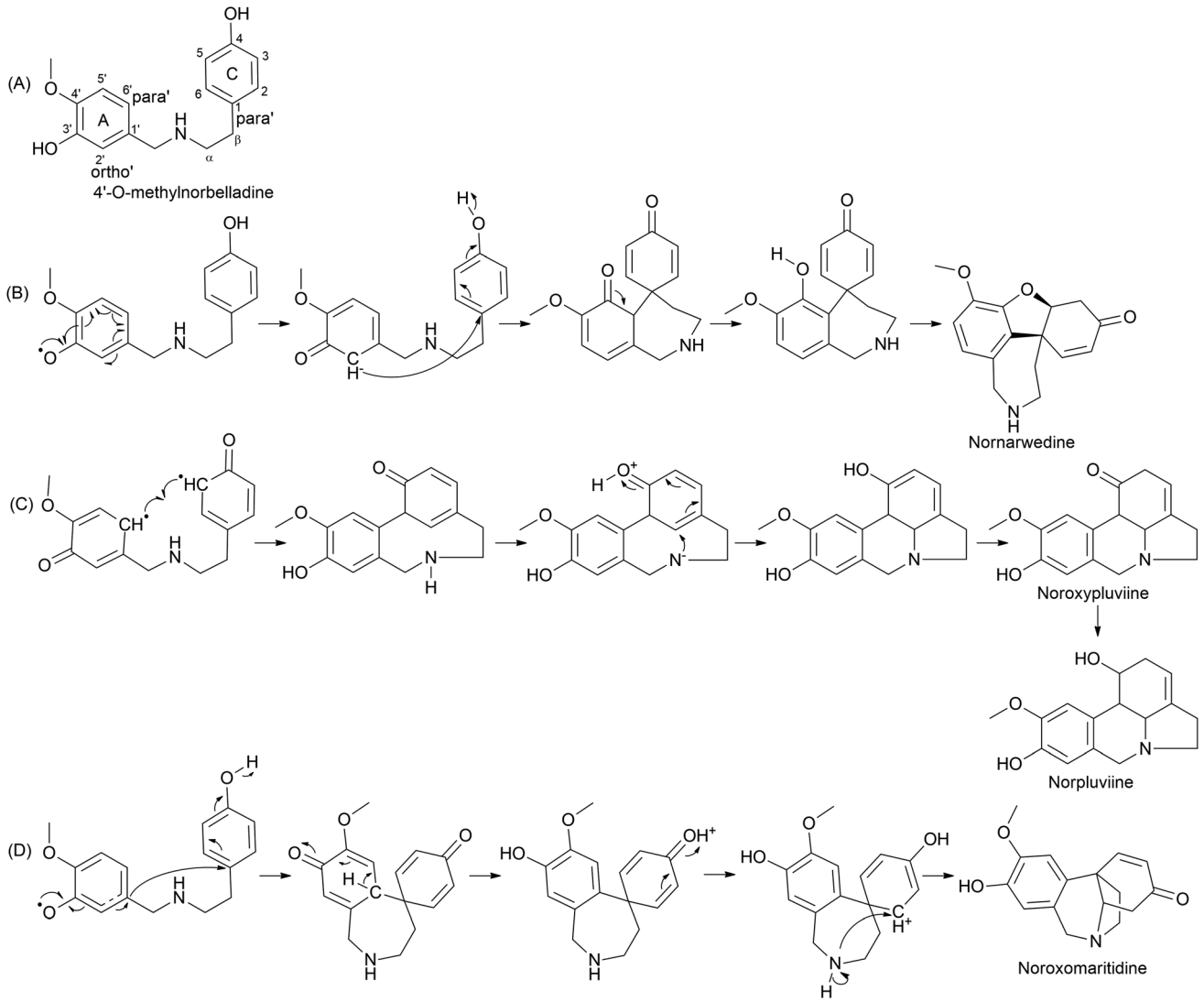

Fig. 5 Proposed mechanism for the phenol coupling reaction. (A) The structure of 4′-*O*-methylnorbelladine; (B) *para*–*ortho*′ coupling leading to nornarwedine; (C) *ortho*–*para*′ coupling resulting norpluviine; (D) *para*–*para*′ coupling leads to noroxomaritidine.

chemical proof of its structure was provided by Hazama *et al.* (1968) through the total synthesis of lycoramine.[72] However, most of the reported synthetic strategies produced galanthamine and lycoramine alkaloids in racemic mixtures. The asymmetric total synthesis of (−)-galanthamine and (−)-lycoramine was published by Chen *et al.* (2012) using a common intermediate of racemic α-aryloxy cyclic ketone to asymmetric hydrogenation and intramolecular reductive Heck cyclization to reach the desired end product.[73] Another approach was reported by Li *et al.* (2015) to successfully obtain the above components through the asymmetric Michael addition of intermediate.[74] A recent publication by Majumder *et al.* (2022) added (−)-narwedine and (−)-lycoraminone to the list by *ortho* ester Johnson–Claisen rearrangement of allyl alcohol.[75]

Sanguinine and childanthine comprise the same dibenzofuran nucleus, confirming their relationship with this pathway. However, either the pathway proceedings to the above or the enzymes involved have not yet been reported or critically analysed.

2.3.2 *Ortho–para′* phenol coupling: lycorine and homolycorine. *Ortho–para′* phenol oxidative coupling results in two distinct alkaloid types, namely, the lycorine-type with a pyrrolo [*de*]phenanthridine skeleton and the homolycorine-type with the 2-benzopirano-[3,4-*g*]indole skeleton (Fig. 7 and 8A). The conversion of 4′-*O*-methylnorbelladine to lycorine and lycorenine has been widely studied with tritium labelling in Amaryllidaceae plants.[67,76–79] These studies indicate that 4′-*O*-methylnorbelladine was initially converted to an intermediate now identified as noroxopluviine, first proposed by Kirby and Tiwari (1966),[79] and further reduced to norpluviine,[80] followed by caranine to lycorine through hydroxylation. *Ortho–para′* phenol coupling is suggested to be followed by stereospecific carbon nitrogen bond formation to establish noroxopluviine (Fig. 5 and 7). However, an achiral/racemic intermediate development is ignored by hypothesizing that a carbon–

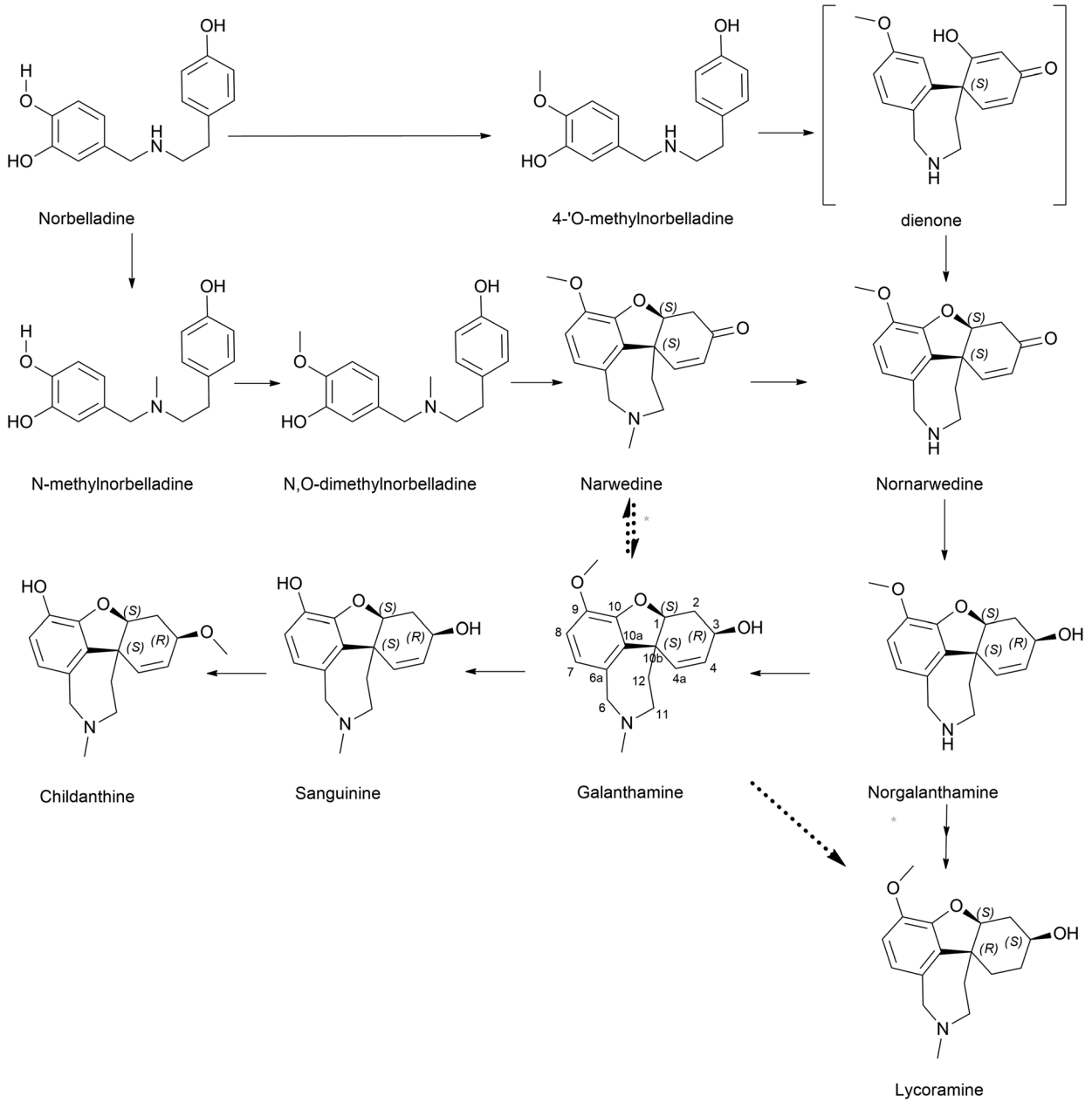

Fig. 6 *Para–ortho′* coupling pathway-related components. Galanthamine is the primary pathway illustrated. Dashed arrows indicate minor controversial steps, where more than one arrow represents multiple steps.

nitrogen bond occurs prior to re-aromatization and/or keto–enol tautomerization.[79] Bruce and Kirby (1968) incorporated tritium labelled tyrosine (3′,5′-$^{3}H_2$), where norpluviine carried over half of them at C2 in *Narcissus*.[76] The radiolabel was then successfully delivered to the lycorine without any loss. This confirms the involvement of position 5 of the C6–C2 unit in the phenol coupling process. However, an inversion of the tritium was observed at C2, suggesting a mechanism linking an epoxide, followed by an allylic rearrangement (Fig. 8).

Furthermore, the double incorporation of tritium and ^{14}C to study norpluviine to lycorine solidified the notion that the hydroxylation process is stereospecific based on isotope label integration ratios. Wildman and Heimer reported similar observations with *Zephyranthes candida*.[78] Interestingly, pluviine-to-galanthine conversion *via* methylpseudolycorine is reported to occur similarly, with inversion at C2.[81] The alkaloid incartine was first identified and proposed as an intermediate of galanthine to narcissidine transformation by Kihara and a team in *L. incarnate*.[82,83] Epoxide formation and the stereospecific C11 loss of hydrogen ultimately result in narcissidine. However, a contradicting view of the retention of configuration 2β-^{3}H in caranine was also reported in *Clivia miniata*.[77] Intriguingly, there was a complete loss of tritium in the original *ortho* position (C3) of the C6–C2 fragment, which leads to an

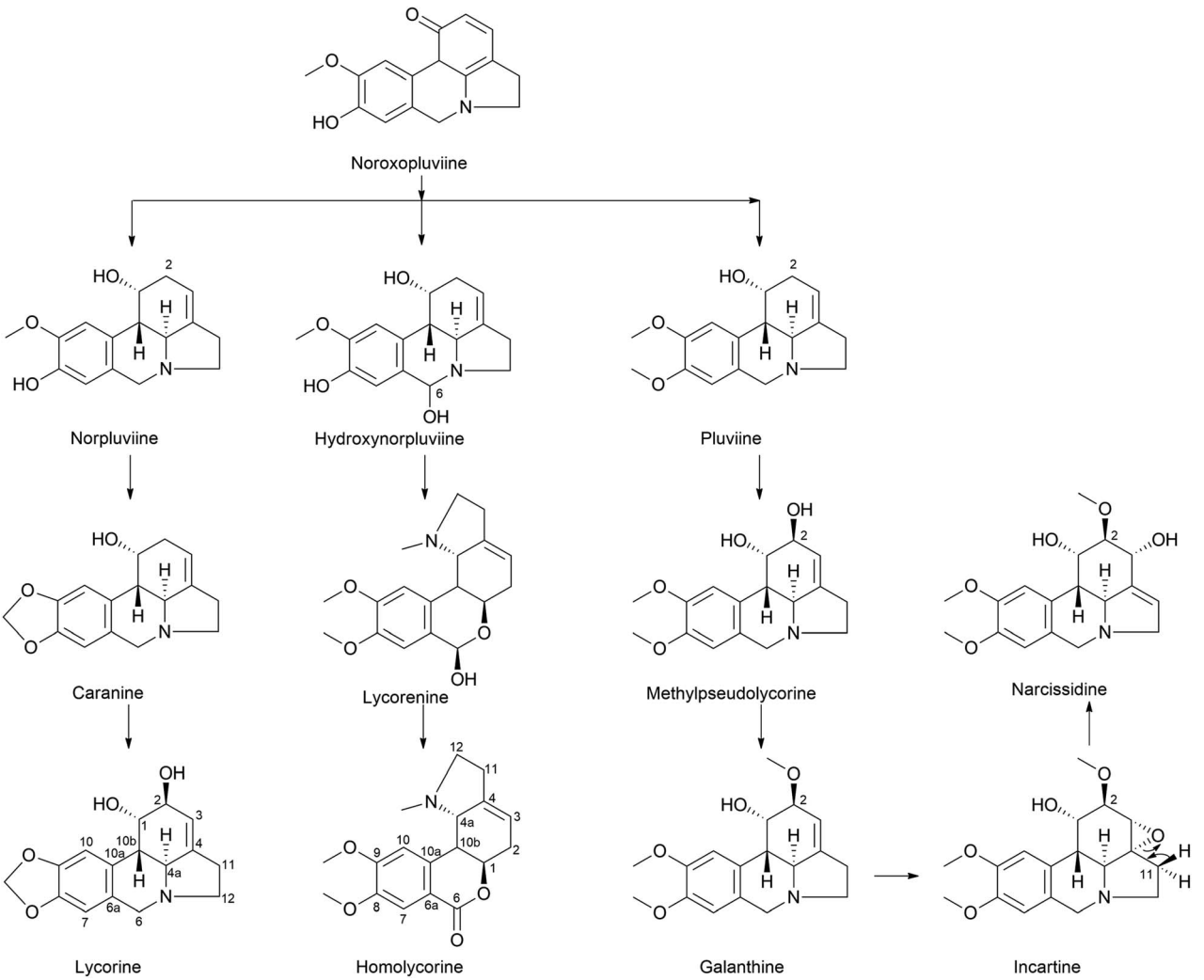

Fig. 7 *Ortho–para′* coupling pathway in lycorine and homolycorine-type alkaloid biosynthesis. Narcissidine biosynthesis through galanthine also illustrated.

altered stereochemical hydroxylation pathway, hence irradicating the implication of the 2-oxo-derivative. It is noteworthy that norpluviine should undergo methylenedioxy bridge formation from *O*-methoxyphenol at the C6–C1 unit and allylic hydroxylation at the C6–C2 unit (C2). This has led to the understanding that norpluviine yields caranine and then lycorine.[80] The structure of lycorine was first determined by Nakagawa *et al.* in 1956, and absolute stereochemistry was assigned.[84,85] Since then, lycorine and its type alkaloids have been investigated because of their structure, bioactivity and relevant relationship although the metabolic pathway involving particular enzymes is yet to be revealed.

The homolycorine pathway derives from different directions initiated from norpluviine by reducing its C6 position to obtain hydroxynorpluviine, and the oxidation of the same leads to a ring opening between C6 and nitrogen. This leaves *ortho–para′* C–C coupling bond vulnerable to free rotation. Consequently, it allows the C6 ketone and C1 hydroxyl groups to create a hemiacetal linkage. However, it is questionable whether ring closure or *O*/*N*-methylation occurs primarily to produce lycorenine. The stereochemistry of lycorenine production from norpluviine was studied by Fuganti and Mazza (1973),[68] where they confirmed the removal of C6 *pro*-R hydrogen by allowing hydroxylation in the final product lycorenine. However, the behaviour of stepwise intermediates is not reported here. Further oxidation of the C6 hydroxyl of lycorenine ultimately results in homolycorine.

2.3.3 *Para–para′* phenol coupling: crinine-, narciclasine-, tazettine- and montanine-types. The *para–para′* oxidative coupling leads to several types of AA increasing diversity. Among these, crinine/haemanthamine-type (5,10*b*-ethanophenanthridine), narciclasine/pancrastatin-type (phenanthridine), tazettine/pretazettine-type (2-benzopyrano[3,4-*c*]indole), and montanine-type (5,11-methanomorphanthridine) skeletons are prominent. In their case, C–C coupling was published, which establishes 2 of 4 possible enantiomers of noroxomaritidine through an achiral intermediate, thus leading to either crinine and/or montanine, pancrastatin, and tazettine skeletons depending on their stereochemistry.[47,70] Crinine is suggested to

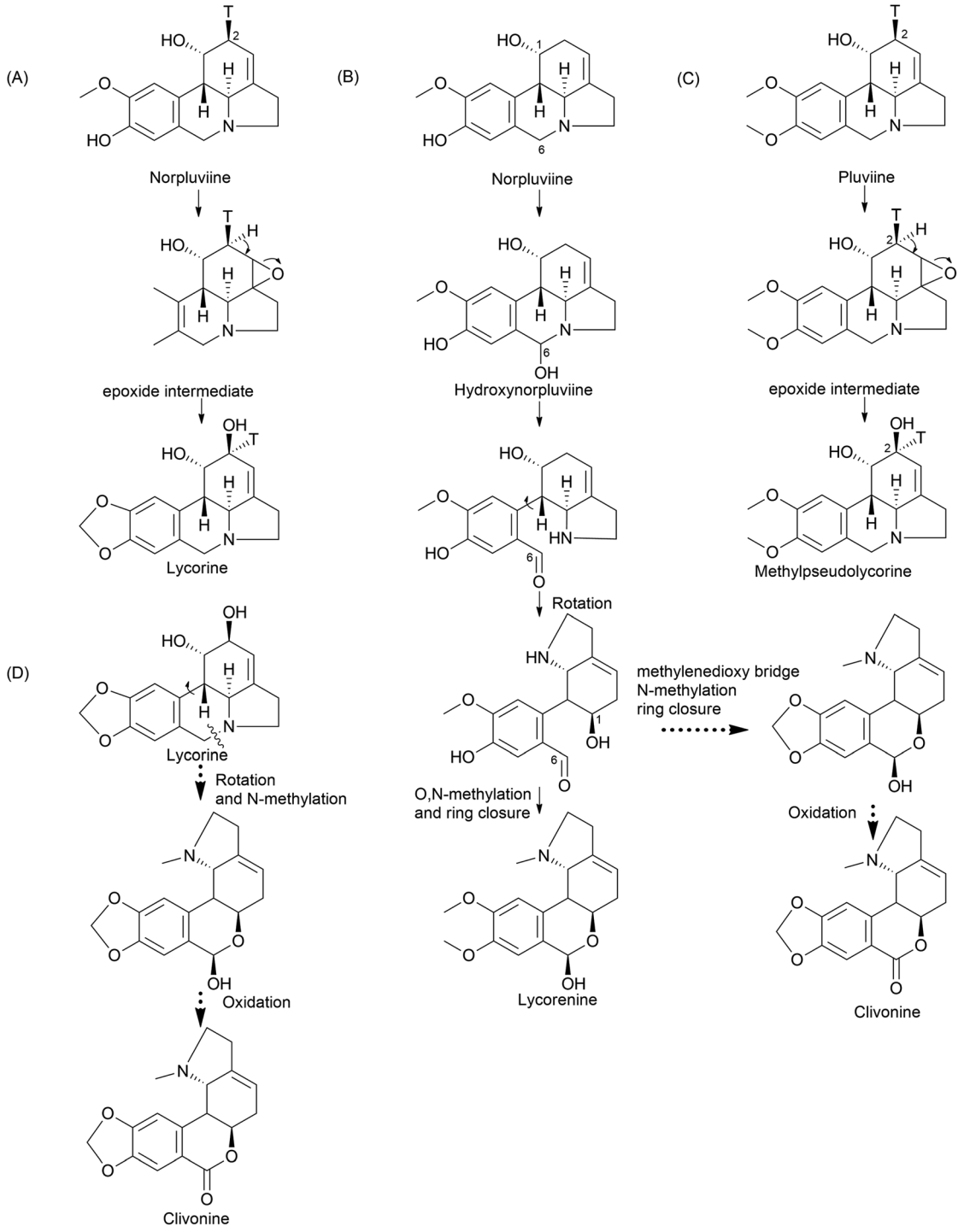

Fig. 8 *Ortho–para′* coupling pathway-related components biosynthetic mechanisms. Norpluviine proceeds to lycorine through (A) inversion and/or retention of C2 tritium elucidates hydroxylation stereospecificity; (B) bond cleavage, rotation, and hemiacetal bond establishment, and another pathway to reach clivonine; (C) suggested epoxide intermediate formation to achieve methylpseudolycorine; (D) clivonine biosynthesis *via* lycorine.

be biosynthesized from (10b*S*,4a*R*)-noroxomaritidine *via* (10b*S*,4a*R*)-normaritidine by conserving its stereochemistry (Fig. 9).[70] However, this requires methylenedioxy bridge formation and possible retention or inversion of the hydroxyl group (C3). Another possibility, established earlier, is that racemic intermediate oxocrinine is generated from noroxomaritidine to yield haemanthamine.[86,87] Thus, it becomes a choice between reduction and oxide bridge formation to occur at the outset. Conversely, vittatine-to-haemanthamine transformation requires hydroxylation and *O*-methylation, which is

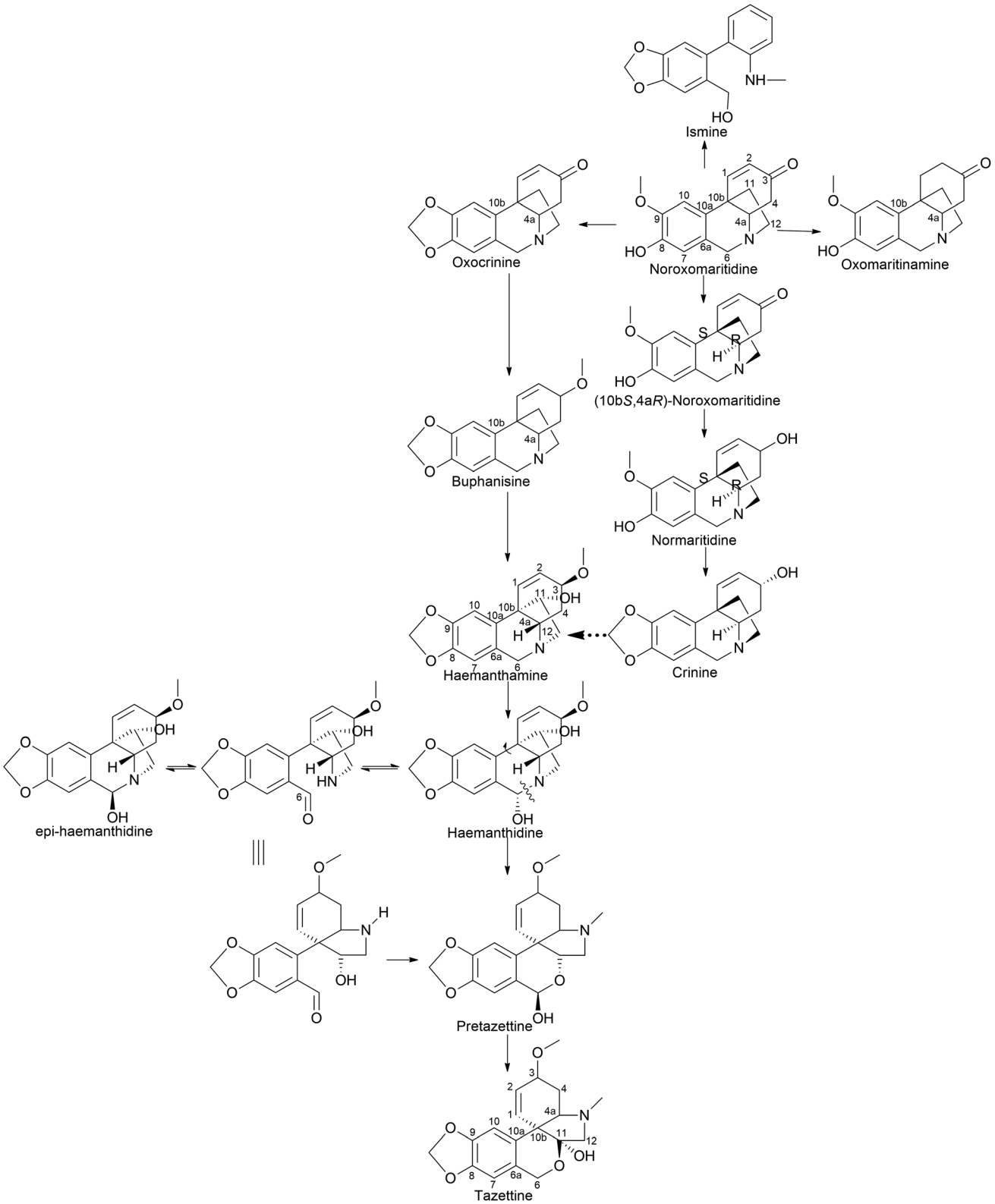

Fig. 9 *Para–para′* coupling to reach crinine and tazettine type skeletons.

hence proposed to be mediated *via* 11-hydroxyvittatine (Fig. 10).[88] The involvement of an enzyme to convert vittatine to 11-hydroxyvittatine, named vittatine 11-hydroxylase (V11H), was investigated although the absolute configuration of the resultant compounds remains unresolved.[89] As initially discussed by Kornienko and Evidente in their 2008 report,[32] narciclasine cannot be classified as an alkaloid owing to its amidic nitrogen. However, it is pertinent to include narciclasine in this

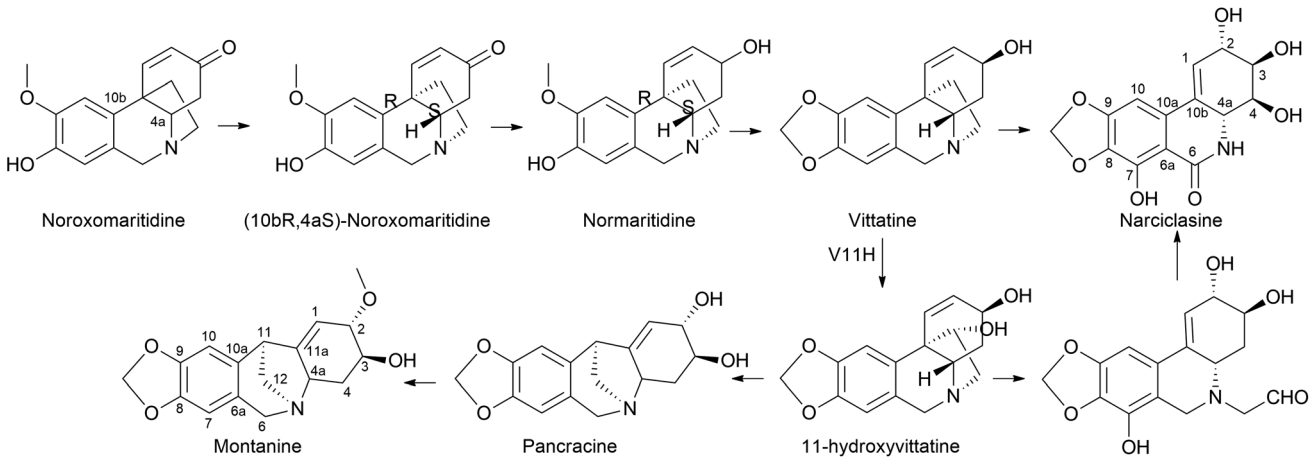

Fig. 10 *Para–para′* coupling to reach narciclasine and montanine type skeletons.

study owing to its striking structural resemblance to Amaryllidaceae lycorine-type alkaloids. Narciclasine in earlier studies was questioned to be derived from *ortho–para′* (lycorine) or *para–para′* (haemanthamine) pathways considering its structural affinity to both lycorine and haemanthamine. The hypothesis was established owing to the frequent identification of alkaloids of both types and narciclasine from the same plants. However, tritium labelled *O*-methylnorbelladine experiments in daffodils have now well established that narciclasine emerges from *para–para′* phenol coupling. The incorporation was investigated in lycorine, haemanthamine, and narciclasine. It was observed that narciclasine retained 75% radiolabelling, while lycorine and haemanthamine were 50% and 100%, respectively. This solidifies the *O*-methylnorbelladine incorporation into narciclasine *via* the *para–para′* branch pathway. Although controversial, narciclasine has also been suggested to arise from 11-hydroxyvittatine following a retro-Prins reaction, losing the ethane bridge and rearrangement (amine oxidation, hydroxylation, and oxidation)[88] (Fig. 10). Simultaneously, biological derivatization of narciclasine from vittatine has also been established by [2,4-$^3H_2$]4′-*O*-methylnorbelladine feeding experiments in *Narcissus* "Twink" and "Texas", where radiolabeled crinine was not incorporated into narciclasine, but vittatine was.[90] The common intermediate property of 11-hydroxyvittatine is further established by its candidacy to convert to haemanthamine, as published by Feinstein and Wildman (1973) using *Rhodophiala bifida* tritium treatment.[91] The route to pretazettine (identified as tazettine) was investigated with tritiated haemanthamine in *Sprekelia formosissima* (L.), revealing the biological sequences to be haemanthamine, haemanthidine, and tazettine[92] (Fig. 9). A subsequent publication stated that pretazettine is a naturally occurring form, while tazettine is an artifact due to the chemical liabilities proven using *Sprekelia formosissima* and *Ismene narcissiflora* large-scale isolation of alkaloids.[93] The interconversion from haemanthidine to pretazettine is mediated through a ring opening between C6 and nitrogen, followed by a ~90° rotation to create a transition stage ketone intermediate.[91] Similar to the lycorenine pathway, hemiacetal formation is observed at the C6 ketone and C11 hydroxyl groups, followed by *N*-methylation. Furthermore, the pathway extends to montanine, sharing the 5,11-methanomorphanthridine nucleus. In an attempt to clarify montanine biogenesis, initial experiments were simulated with tritiated haemanthamine in *Haemanthus coccineus*, but no alkaloids corresponding to montanine were radiolabelled. This suggests that the C3 methoxy group in haemanthamine might interfere with the transformation. The study was repeated in *Rhodophiala bifida* altering tritiated supplement to vittatine, as it was previously reported to house vittatine, 11-hydroxyvittatine, haemanthamine and montanine, among other alkaloids. It was observed that a radiolabel was performed for both haemanthamine and montanine. Thus, the path proposed vittatine to be converted to 11-hydroxyvittatine, pancracine, and finally produce montanine.[91]

It is surprising that irrespective of the widely elaborated structural diversity studies on the pathway of AA after phenol coupling reactions, only few biosynthetic evaluation attempts have been made to reveal the enzymes involved. Kilgore *et al.* (2016) for the first time published on CYP96T1 can produce two out of four enantiomers of noroxomaritidine [(10b*R*,4a*S*) and (10b*S*,4a*R*)] from 4′-*O*-methylnorbelladine, thus exhibiting its potential in *para–para′* direction. However, minor amounts of nornarwedine were also observed, opening the pathway towards *para–ortho′* direction. It was reported to be the first phenol coupling enzyme to be characterized from a monocot. It is noteworthy that CYP96T1 also converted 4′-*O*-methyl-*N*-methylnorbelladine to produce several C–C phenol-coupled products, with narwedine being one of them (Fig. 5). Interestingly, no product formation was observed when 3′-*O*-methylnorbelladine was fed as the substrate.[70] The same team reported noroxomaritidine reductase (NR) (discussed in Subsubsection 2.2.1 as norcraugsodine reductase) for its involvement in the conversion of noroxomaritidine to oxomaritinamine[47] (Fig. 9).

Barton proposed a novel concept that extended the scope of intermolecular phenolic coupling to form tazettine and lycorenine subclasses.[69] This involved rearranging haemanthamine and lycorine-type precursors through a process referred to as "ring switching" by Giró Mañas *et al.* (2010).[94] Wildman later

confirmed these theories through tritium feeding experiments in *Sprekelia formosissima*, supporting the formation of tazettine, and in *Narcissus* 'King Alfred' for lycorenine considered earlier.[78,95] Wildman introduced a biomimetic procedure for generating pretazettine from haemanthidine. However, challenges were encountered in developing an analogous protocol for the biomimetic conversion of lycorine into lycorenine-type ring systems. The transformation necessitates a ~180° rotation and involves minimal strain relief unlike the ~90° rotation with significant strain relief observed in the haemanthidine/pretazettine series.[81,96] Consequently, Barton's original hypothesis remained unconfirmed from a synthetic perspective until Giró Mañas *et al.* (2010)[94] finally corroborated experimentally the biogenetic hypothesis.

Clivimine classification in the literature is a subject of contention, with some scientists categorizing it as an independent ring structure,[32] while most assert it belongs to the lycorenine subclass.[94,97,98] Clivonine, a compound first isolated and characterized from *Clivia miniata* Regel in 1956 by Wildman,[99] shares the same core ring system (2-benzopyrano[3,4-*g*] indole) as lycorenine-type alkaloids albeit with a slight modification involving methylenedioxy bridge formation from *O*-methoxyphenols at the C6–C1 unit and lactol oxidation at C7. The biosynthesis of clivonine from a lycorine-type progenitor necessitates benzylic oxidation, a ~180° ring switch, followed by *N*-methylation and lactol oxidation.[94]

Limited information is available regarding the mechanistic aspects of the catabolic pathway that lead to ismine. Fuganti (1973)[100] reported feeding experiments conducted to elucidate certain stereochemical aspects of this biosynthetic process. *Sprekelia formosissima* was used [6,10-$^{3}H_2$; 12-^{14} C] noroxomaritidine for labelling, which resulted in incorporations of 0.03% into ismine, 2% into haemanthamine, and 0.8% into haemanthidine. Ismine showed no ^{14}C activity. The radioactive ismine's labelling pattern was indirectly determined by its conversion into phenanthidone, which retained approximately 25% of the tritium activity. This suggests that during the biological transformation of noroxomaritidine into ismine, there is a loss of the original tritium located at C-6 in noroxomaritidine, specifically at the benzylic position adjacent to tertiary nitrogen, a stereospecific removal of hydrogen at some point in the biosynthesis, followed by a reduction step. Furthermore, the complete absence of 14C activity indicates that the carbon atom at C-1 of [6,10-$^{3}H_2$; 12-^{14}C]noroxomaritidine is not retained as an *N*-methyl group in ismine. Hence, the report suggests that ismine is derived through *para–para* coupling, followed by late elimination of the ethanol bridge from the C-15 crinane skeleton.

3 Recently reported anti-viral activities of Amaryllidaceae alkaloids and their possible molecular targets

Amaryllidaceae are recognized for their therapeutic properties[24] owing to the isoquinoline alkaloids they produce.[23] In addition to their probable endogenous role in the protection against plant foreign invaders,[101] AA possess multiple biological properties relevant to human health. For example, galantamine is a strong inhibitor of acetylcholinesterase and has been approved for treating mild symptoms of Alzheimer's disease. Other AAs display anti-microbial properties against various animal and human threats. The first available report on the antiviral properties of alkaloids dates back to 1976 by Furusawa *et al.*,[102] and impressively, the discovery of new antiviral activities has been unceasing. In 1989, Renard-Nozaki and colleagues showed that several types of AA target the herpes simplex virus, a DNA virus.[103] In 1992, Gabrielsen *et al.* uncovered that many AAs also impede the replication of several families of RNA viruses *in vitro*, and in a mouse model.[104] Lycorine has emerged as one of the most efficient antiviral compounds of this family, targeting a broad range of virus types at nM concentrations. The last 5 years have been scarred by the Coronavirus Disease 2019 (COVID-19) pandemic, orienting research towards the discovery of anti-severe acute respiratory syndrome coronavirus 2 (SARS-CoV-2) molecules. In this section, recent discoveries on AA antiviral activity against coronaviruses but also against other emerging or reemerging diseases impacting human health (such as dengue, Zika, influenza and chikungunya viruses); or animals (duck tembusu virus, DTMV); and plants (tobacco mosaic virus, TMV) are summarized (Table 1).

3.1 Severe acute respiratory syndrome coronavirus 2 (SARS-CoV-2)

Lycorine was reported to exhibit anti-coronaviral activities in 2005.[105] In the early days following the onset of the COVID-19 pandemic, Zhang *et al.* tested the antiviral properties of SARS-CoV-2 permissive VeroE6 cells (isolated from the kidney of an African green monkey) and human hepatocarcinoma-derived Huh7 cells.[106] They showed that lycorine EC_{50} (compound concentration required to inhibit 50% of viral titer) was 0.31 μM (assessed at 72 h), with a CC_{50} > 40 μM (concentration required to kill 50% of the cells, assessed at 24 h in this case). In 2021, Jin and colleagues further investigated its mechanism of action. They first confirmed its anti-coronaviral effect against SARS-CoV, SARS-CoV-2 and MERS-CoV (Middle East Respiratory Syndrome – CoV) with slightly higher EC_{50} (1.021, 0.878, and 2.123 μM, respectively), (Table 1). Their results suggested that lycorine blocked RNA replication, acting as a non-nucleoside RNA-dependent RNA polymerase inhibitor (RdRp) of MERS-CoV with a measured IC_{50} of 1.406 μM.[6] Their docking analysis demonstrated that lycorine also interacted with SARS-CoV-2 RdRp through hydrogen bonding with Asp623, Asn691, and Ser759 residues. In 2021, Ren *et al.* used a muti-targeting approach including both computational and experimental techniques to assess the potential of three alkaloids to tackle SARS-CoV-2 replication and clarify the lycorine effect on SARS-CoV-2 replication.[2] First, they predicted that lycorine may target the host cell 80S ribosome subunit by applying computational methods. To reach this conclusion, the authors constructed a three-dimensional *in silico* model of the human ribosome in a complex with lycorine using the experimental structure of yeast ribosomes complexed with lycorine as a reference. The AA was found to fit tightly into the ribosome

Table 1 Summary of recent studies on Amaryllidaceae alkaloid antiviral effect[a]

	Virus	Alkaloid EC_{50}, CC_{50}	Target (IC_{50})	Model	Ref.
Coronavirodeae	SARS-CoV	Lycorine (EC_{50} = 0.31 μM, CC_{50} > 40 μM)	n.d.	*In cellulo* (simian VeroE6 and human Huh7 cells)	106
		Lycorine (EC_{50} = 1.02 μM; CC_{50} > 10 μM)	n.d.	*In vitro* + *in cellulo* (Vero)	8
	SARS-CoV-2	Lycorine (EC_{50} = 0.878 μM; CC_{50} > 10 μM)	*In silico* docking with RdRP	*In vitro* + *in cellulo* (Vero)	8
		Lycorine (EC_{50} = 0.439 μM, CC_{50} > 1000 μM in VeroE6, 0.834 μM in Huh7, 1.044 μM in HEK293T cells)	(1) Ribosome (*in silico*), (2) binding to frameshift stimulation element (FSE) in SARS-CoV-2 genome (*in silico*), (3) RdRp (*in silico* and *in vitro*), (4) viral core assembly (*in vitro*)	*In silico*, *in vitro* and *in cellulo* (VeroE6, Huh7, HEK293T)	2
		Lycorine (EC_{50} = 0.01 μM, CC_{50} = 18.78 μM)	M^{Pro}	*In vitro* (cell protease assay)	4
		*Tran*s-dihydrolycoricidine (EC_{50} = 0.18 μM, CC_{50} = 3.48 μM), dihydronarciclasine analog with ring-A mono-substituted C7-OH (EC_{50} = 0.09 μM, CC_{50} = 1.92 μM)	n.d.	*In cellulo* (Calu3)	14
	MERS-CoV	Lycorine (EC_{50} = 2.123 μM; CC_{50} > 10 μM)	RdRp ($IC_{50=}$ 1.406 μM)	*In vitro* (cell-based reporter assay), *in cellulo*	8
Flaviviridae	ZIKV	Hippeastrine hydrobromide (EC_{50} = 3.62 μM; CC_{50} > 100 μM)	Post-entry	*In cellulo* (hNPCs, human fetal-like forebrain organoids), *in vivo* (adult mouse)	109
		Lycorine (EC_{50} = 0.22–0.39 μM; CC_{50} = 4.4–21 μM)	Post-entry step during RNA replication, RdRp (IC_{50} = 25 μM)	*In cellulo* (A549, Huh7 and Vero), *in vivo* AG6 mice (10 mg kg^{-1})	110
		Cherylline (EC_{50} = 20.3 μM; CC_{50} > 100 μM)	Post-entry step – RNA synthesis	*In cellulo* (VeroE6 and Huh7)	111
		Lycorine (EC_{50} = 0.9 μM; CC_{50} = 4.3 and 3.4 μM in BHK-21 and Vero), pretazettine (1.9 μM; CC_{50} = 5.4 and 7.2 μM), narciclasine (EC_{50} = 0.02 μM; CC_{50} = 0.09 and 0.12 μM), narciclasine-4-*O*-β-D-xylopyranoside (EC_{50} = 7.9 μM; CC_{50} = 39.3 and 51.8 μM)	n.d.	*In cellulo* (BHK-21 and Vero)	112
	DENV	Cherylline (EC_{50} = 8.8 μM; CC_{50} > 100 μM)	Post-entry step – RNA synthesis	*In cellulo* (VeroE6 and Huh7.5)	111
		Haemanthamine (EC_{50} = 337 nM; CC_{50} > 10 μM), pancracine (EC_{50} = 357 nM; CC_{50} > 10 μM) haemanthidine (EC_{50} = 476 nM; CC_{50} > 10 μM)	n.d.	*In cellulo* (Huh7)	1
		3,4-Dihydroxybenzaldehyde (EC_{50} = 24.1 μM; CC_{50} = 173.1 μM), 3′,4′-*O*-dimethylnorbelladine (EC_{50} = 27.5 μM; CC_{50} = 131.4 μM), norcraugsodine (EC_{50} = 37.7 μM; CC_{50} = 121.8 μM)	n.d.	*In cellulo* (Huh7)	3
		Lycorine (EC_{50} = 0.9 μM), pretazettine (EC_{50} = 1.9 μM), narciclasine (EC_{50} = 0.02 μM), narciclasine-4-*O*-β-D-xylopyranoside (EC_{50} = 7.9 μM)	n.d.	*In cellulo* (BHK-21 and Vero)	112
	DTMUV	Lycorine (EC_{50} = 2 μM)	Post-entry step	*In cellulo* (BHK-21)	113
Orthomyxoviridae	INFV	Lycorine (EC_{50} = nd)	Nuclear–cytoplasmic transport impairment, decrease Nup93 expression	*In cellulo* (GD178 and MDCK)	114 and 115

Table 1 (*Contd.*)

	Virus	Alkaloid EC_{50}, CC_{50}	Target (IC_{50})	Model	Ref.
		Lycorine ($EC_{50=}$nd)	Blockage of nuclear export of vRNP through repression of COX41 and ERK signaling pathway	*In cellulo* (MDCK), *in vivo* (in mice 5 mg kg^{-1} day^{-1})	115
Togaviridae	CHIKV, SINV, SFV, and VEEV	Lycorine (EC_{50} = 0.38–0.75 μM, CC_{50} > 10 μM); SINV, SFV, and VEEV (1.05, 0.83 and 0.31 μM)	Post-entry – viral translation	*In cellulo* (Vero, BHK21, Huh7, A549)	9
Picornaviridae	EV71 and CVA16	LY-55 (2-hydroxy-2,3*a*1,4,5,7,12*b*-hexahydro-1*H*-[1,3]dioxolo[4,5-*j*] pyrrolo[3,2,1-*de*]phenanthridin-1-yl 2-((4-fluorophenyl)thio)acetate hydrochloride) (EC_{50} = 1.69–5.01 μM, CC_{50} = 106.36 μM)	Not virucidal, blocking autophagy	*In cellulo* (Vero) and *in vivo* (mice)	6
Herpesviridae	HSV	Dihydronarciclasine analog with ring-A mono-substituted C7-OH (EC_{50} = 0.209 to 0.504 μM, and no impact on viability <50 μM) *trans*-dihydrolycoricidine (EC_{50} = nd)	(1) Activation of ERK, ElF2 and PKR; (2) integrated stress response; (3) autophagy; (4) sirtuin signaling pathways; (5) innate antiviral response	*In cellulo* (in organoids with hiPSC), *in vivo* (mouse)	14
Tobamoviridae	TMV	Lycorine (EC_{50} = nd)	Uncharacterized	*In planta*	116
		Lycoricidine derivatives (*N*-methyl-2,3,4-trimethoxylycoricidine), (*N*-methyl-2-methoxy-3,4-acetonidelycoricidine) (EC_{50} = nd)	Triggers defense enzyme activity	*In planta*	117

[a] SARS-CoV: severe acute respiratory syndrome – coronavirus, MERS-CoV: middle east respiratory syndrome – coronavirus, DENV: dengue virus, ZIKV: Zika virus, WNV: West Nile Virus, DTMUV: duck tembusu virus, INFV: influenza virus, CHIKV: chikungunya virus, SINV: Sindbi Virus, SFV: Semiliki Forest Virus, HSV: Herpes Simplex Virus, TMV: tobacco mosaic virus. RdRp: RNA-dependent RNA polymerase. M^{Pro}: SARS-CoV main protease. RNP: ribonucleoprotein. N.d.: not determined.

peptidyl transfer site and was stabilized by hydrogen bonds with several amino acids and Mg^{2+}. Second, they suggested that lycorine attenuates SARS-CoV-2 propagation by binding to the frameshift stimulation element (FSE), which is a structured RNA motif from the SARS-CoV-2 genome with a 5′ heptanucleotide slippery site UUUAAAC and a three-stem pseudoknot involved in polyprotein processing.[107] Their prediction demonstrates that lycorine binds near the slippery site of this viral RNA structure. Further computational analysis coupled with *in vitro* binding affinity data predicted that lycorine may also inhibit RNA synthesis by occupying the RNA growth site of RdRp but only in the presence of RNA. Lycorine was too small a molecule to sojourn in the RdRp large empty cavity in its apo state but could be stabilized following binding with RNA, as the enzyme cavity becomes more compact. In this sense, the affinity of lycorine for the enzyme might be secondary to its affinity to nucleic acids. Finally, in experimental settings of cell infection, an EC_{50} of 0.438 μM was measured by RT-qPCR in VeroE6 cells, and an unexpected CC_{50} > 1000 μM. However, lycorine notorious cytotoxicity was detected in human hepatocarcinoma Huh7 and human embryonic kidney HEK293T cells, with much lower CC_{50} of 0.834 and 1.044 μM, respectively. In 2022, Narayanan *et al.* indicated that lycorine may also target SARS-CoV-2 polyprotein processing through the inhibition of main protease (M^{Pro}) activity in a cell protease assay although no interaction with key residues in the catalytic site of the enzyme could be detected by docking analysis.[4] Although many recent studies have focused on lycorine, narciclasine and its analogues have been previously shown to be strong inhibitors of coronaviruses and RNA viruses possibly through interaction with eukaryotic translation elongation factors eEF1A, nucleocapsid and/or nucleic acids, as extensively reviewed in.[108] Earlier this year (2023), chemically synthetized *trans*-dihydrolycoricidine and dihydronarciclasine analog with ring-A mono-substituted C7-OH were also identified as inhibitors of SARS-CoV-2,[14] with IC_{50} = 0.18 μM, CC_{50} = 3.48 μM, IC_{50} = 0.09 μM, and CC_{50} = 1.92 μM. Le *et al.* reported that 6α-hydroxyhippeastidine, 6β-hydroxyhippeastidine, 2-*epi*-lycorine, zephyranthine, and ungeremine isolated from *Hymenocallis littoralis* demonstrated weak anti-SARS-CoV-2 activity.[109] Unfortunately, none of these studies tested the efficacy of lycorine or other AAs in animal models of SARS-CoV-2 infection, but they add to the evidence that some AAs are potent antiviral compounds against emerging coronavirus infections and that they probably target multiple steps of the viral replication cycle.

3.2 Dengue and Zika viruses

Dengue fever, caused by the dengue virus (DENV), is the most prevalent arthropod-borne viral disease and is endemic to tropical and subtropical regions, progressively affecting temperate regions. Zika virus (ZIKV), a closely related flavivirus,

can be transmitted vertically *in utero* and causes congenital Zika syndrome, other birth defects, and Guillain–Barré syndrome in adults. No approved antiviral drugs for these diseases are currently available. As early as 1992, Gabrielsen *et al.* detected that some AAs could inhibit flaviviruses, such as the Japanese encephalitis virus, the yellow fever virus, and DENV.[104] In recent years, many studies have contributed to increasing our knowledge of the anti-flaviviral properties of AAs. In 2017, Zhou and colleagues reported that hippeastrine hydrobromide (HH) inhibited ZIKV infection at a post-entry step in human pluripotent stem cell-derived cortical neural progenitor cells (hNPCs) (EC_{50} = 3.62 μM, Table 1).[110] They further showed that treatment with 25 μM of HH for 3 and 17 days rescued ZIKV-induced growth and differentiation defects in hNPCs and human fetal-like forebrain organoids and that it efficiently inhibited ZIKV infection in adult mouse brains *in vivo*. HH suppressed viral propagation when administered to adult mice with active ZIKV infection (at a dose of 100 mg kg^{-1} day^{-1} subcutaneously). The authors concluded that HH is a highly promising drug candidate for treating ZIKV-infected patients. In 2020, Chen *et al.* aimed to elucidate the anti-ZIKV properties of lycorine.[111] They used RT-qPCR, immunofluorescence, western blot, and plaque forming assay to analyze viral RNA (vRNA), viral protein, and progeny virus counts in A549, Huh7 and Vero cells. The time-of-drug addition assay suggested that the AA acts at a post-entry step during RNA replication with EC_{50} ranging from 0.22 to 0.39 μM and CC_{50} ranging from 4.4 to 21 μM. The authors also showed that lycorine increased the thermal stability of NS5 (containing RdRp and methyltransferase domains) and that RdRp activity was reduced by 50% when the enzyme was treated with 25 μM of the compound. However, at this concentration, lycorine is highly cytotoxic to human cells mitigating the relevance of this interaction. Finally, the authors showed that treatment with lycorine (10 mg kg^{-1}) protected AG6 mice against ZIKV-induced lethality (83% less death) by decreasing the viral load in the blood. These results differ from those of previous studies on the West Nile Virus, a related flavivirus in which lycorine does not target RdRp.[112] Instead, its antiviral properties are specific to the 2K peptide, which plays a key role in the replication complex and polyprotein processing.

In 2021, our group uncovered that extracts from Senegalese *Crinum jagus* inhibited DENV infection and that cherylline was a potent anti-flaviviral AA, targeting both DENV (EC_{50} = 8.8 μM) and ZIKV replication (EC_{50} = 20.3 μM).[5] Further experiments revealed that cherylline and lycorine targeted a post-entry step, specifically hindering the viral RNA synthesis step but not viral translation. The cherylline ring structure is distinct from that of lycorine (Fig. 1), and their molecular targets probably differ although both inhibit a post-entry step related to RNA synthesis. *In silico* reverse screening predicted that human cellular proteins, such as estrogen and dopamine receptors, could be targets of cherylline.

In previous studies, we found that alkaloid extracts from another Senegalese Amaryllidaceae, *Pancratium trianthum*, were highly effective in blocking $DENV_{GFP}$ replication[5] although the isolated molecules were not individually tested. We later characterized the activity of several alkaloids isolated from *P. maritimum*, namely lycorine, 9-*O*-demethyllycorine, haemanthidine, haemanthamine, 11-hydroxyvittatine, homolycorine, pancracine, obliquine, tazettine and vittatine.[1] All the tested AA inhibited DENV replication (EC_{50} ranges from 0.34 to 73.59 μM) at low or non-cytotoxic concentrations (CC_{50} ranges from 6.25 μM to >100 μM), haemanthamine (EC_{50} = 337 nM), pancracine (EC_{50} = 357 nM) and haemanthidine (EC_{50} = 476 nM) being the most potent anti-DENV inhibitors. Haemanthamine-type alkaloids are known to target other RNA viruses and retroviruses. Although the mechanism of anti-flaviviral activity has not been studied, previous studies have shown that haemanthamine targets the ribosome peptidyl transferase center A-site on the large ribosomal subunit through interactions with 25S rRNA to disrupt the protein synthesis elongation phase and cancer cell growth.[113] This interaction could lead to the inhibition of viral protein synthesis and block viral replication.

In 2022, we studied the anti-DENV activity of norbelladine, its derivatives and its precursors.[3] We revealed that the 3,4-dihydroxybenzaldehyde (selectivity index (SI) = 7.2), 3′,4′-*O*-dimethylnorbelladine (SI = 4.8), 4′-*O*-methylnorbelladine (SI > 4.9), 3′-*O*-methylnorbelladine (SI > 4.5), and norcraugsodine (SI = 3.2) reduced DENV infection with EC_{50} values ranging from 24.1 to 44.9 μM, and the mechanism of action is currently under investigation. Barbosa *et al.* searched for plant-derived antiviral agents against DENV and ZIKV.[114] Hippeastrum extracts were highly antiviral. Lycorine (0.5 and 0.9 μM), pretazettine (0.8 and 1.9 μM), narciclasine (0.02 and 0.02 μM), and narciclasine-4-*O*-β-D-xylopyranoside (7.5 and 4.9 μM) were identified as anti-DENV-2 and -ZIKV inhibitors although they were also cytotoxic. These results agree with previous studies,[104] suggesting that optimization of the AA structure could lead to new therapeutic strategies to fight flaviviral infectious diseases.

3.3 Duck tembusu virus (DTMUV)

DTMUV is a mosquito-borne flavivirus discovered in 2010 in China 114 and is responsible for fatal outbreaks in ducks[115–117] and other bird species in China and Southeast Asia. Despite the availability of efficient vaccines, outbreaks continue to occur, weighing heavily on the farming economy. In 2021, Lv *et al.* investigated lycorine ability to inhibit the infection of this avian flavivirus.[118] As viral target cells, they used hamster cell lines BHK-21 and evaluated DTMUV replication by real-time PCR, virus titer, western blot and immunofluorescence (IFA) assays. Upon treatment with 5 μM of lycorine (associated with weak cytotoxicity), the authors showed that DTMUV viral titers and envelope protein expression were reduced. Their results are consistent with lycorine targeting a post-entry step, as observed in the context of infections with other flaviviruses or with coronaviruses. The authors also concluded that lycorine is virucidal and blocks viral entry and internalization. Lycorine previously reported that interaction with RdRp, RNA and/or ribosomes could be implicated in DTMUV inhibition. Although the cell line may not be the best representative of DTMUV avian infection, their results suggest that the lycorine structure could serve as a scaffold for the development of new treatments against this disease.

3.4 Influenza virus

In 2013, AA lycorine, hippeastrine, heamanthamine and 11-hydroxyvittatine were reported to display anti-influenza virus type A (A/Chicken/GuangDong/178/2004 (H5N1)) activity at a post-entry step, inhibiting nuclear-to-cytoplasmic export of ribonucleoprotein (RNP).[119] Recent efforts have focused on elucidating the mechanism of action of lycorine.[120,121] In 2019, Yang and colleagues performed a proteomic analysis using a multiplexed tandem mass tag approach to identify changes in protein expression in Madin–Darby Canine Kidney cells infected with H5N1 for 1 hour and treated with 0.52 μM lycorine for 12 hours. The expression levels of 71 proteins were significantly modulated when comparing virus-infected/mock with virus-infected/lycorine-treated cells. Interestingly, influenza virus infection triggered the expression of nuclear pore complex protein 93 (Nup93), while lycorine treatment decreased it. This was confirmed by western blot. Their results endorsed lycorine association with nuclear–cytoplasmic transport impairment, providing new insights into how lycorine may trap viral ribonucleoprotein (RNP) in the nucleus, an inhibitory mechanism of lycorine that appears specific to the context of influenza virus infection (Table 1). In 2022, He and colleagues showed that lycorine might have yet another target.[121] They first identified that the endogenous cytochrome c oxidase subunit 4 isoform 1 (COX41) cellular protein plays an important role in H5N1 infection, promoting viral replication. Intriguingly, when this gene was knocked out, H5N1 RNPs were retained in the cell nucleus, similar to the effect of lycorine on infected cells. They further showed that treatment of cells with 0.52 μM of lycorine inhibited COX41, reducing radical oxygen species levels and phosphorylation of extracellular signal-regulated kinase (ERK), which resulted in the blockage of nuclear export of vRNP and inhibition of viral replication. Continuous treatment with lycorine did not lead to the emergence of a resistant virus. The authors then administered mice with 5 mg kg^{-1} day^{-1} lycorine or mock 1 day prior to viral challenge (2 LD_{50}) and for the remaining 16 consecutive days. On day 5 or 14 post-infection, they observed a reduction in viral titers and inhibition of pathological changes in the lung and trachea tissues. Altogether, these results show that, as is the case for other viruses, lycorine anti-influenza properties might be the consequence of multiple targets and confirm that AA is a potential therapeutic target for the influenza virus.

3.5 Chikungunya virus and other alphaviruses

Chikungunya is a critical re-emerging pathogen caused by a mosquito-borne alphavirus (CHIKV) within the *Togaviridae* family. Other arboviruses of this family include Sindbis virus (SINV), Semliki Forest virus (SFV), which mainly targets rodents, and Venezuelan equine encephalitis virus (VEEV), which affects horses, donkeys and zebras. Li *et al.* investigated whether lycorine and some derivatives could block the replication of these alphaviruses.[9] They observed that lycorine impeded CHIKV with EC_{50} values of 0.38, 0.75, 0.41 and 0.4 μM in Vero, BHK-21, Huh7 and A549 cells, respectively (Table 1). At 10 μM (with some cytotoxicity), CHIKV viral titers were decreased by 10^3–10^5 fold. The authors later showed that lycorine inhibited the replication of SINV, SFV, and VEEV with EC_{50} values of 1.05, 0.83 and 0.31 μM, respectively. They investigated the alkaloid mode of action and convincingly showed that a post-entry step of the CHIKV life cycle was targeted, mainly viral translation, similar to some viruses (SARS-CoV-2), but not to others (DENV, ZIKV, and INFV). Several previously reported mechanisms of lycorine antiviral activity, such as its affinity to RNA and/or ribosome, could affect viral translation. Their results extended the antiviral spectrum of lycorine (Fig. 11).

3.6 Picornaviridae

Human Enterovirus 71 (EV71) and Coxsackievirus A16 (CVA16) are RNA viruses mostly affecting children below 5 years old, causing hand, foot and mouth disease.[122] Lycorine was shown to inhibit EV71 replication *in cellulo* and in animal models in previous studies.[123] In 2019, Wang *et al.* showed that a lycorine derivative LY-55 (2-hydroxy-2,3*a*1,4,5,7,12*b*-hexahydro-1*H*-[1,3]dioxolo[4,5-*j*]pyrrolo[3,2,1-*de*]phenanthridin-1-yl 2-((4-fluorophenyl)thio)acetate hydrochloride) inhibited EV71 and CVA16 with EC_{50} ranging from 1.69 to 5.02 μM, and TC_{50} of 106.36 μM[7] (Table 1). They determined that LY-55 inhibited the autophagy induced by the two viruses and was required for their replication. Alternatively, lycorine was also shown to modulate the Wnt/β-catenin pathway, which has been implicated in the replication of several RNA viruses, such as flavivirideae hepatitis C virus and enterovirus.[124] Finally, the authors showed that treatment of mice with LY-55 (1.5 mg kg^{-1}) decreased viral titers and reduced the mortality rate associated with the lethal EV71 challenge, protecting 4 out of 8 mice from death.[7]

3.7 Herpes simplex virus (HSV)

Herpes Simplex Virus (HSV) is a DNA virus. In 2018, Brown *et al.* developed 10b-aza-analogues of *trans*-hydronarciclasine and *trans*-hydrolycoricidine with B/C-ring fusion-modified derivatives, which completely lost their anti-HSV activity.[13] In 2023, McNulty *et al.* confirmed that dihydronarciclasine analogs and *trans*-dihydrolycoricidine blocked HSV-1 replication.[14] Two derivatives (at 10 μM) displayed strong inhibition of HSV-1 infection in the brain organoids. The dihydronarciclasine analog with ring-A mono-substituted C7-OH was particularly potent (EC_{50} = 0.504 μM in 9001 and 0.209 μM in 01SD organoids with no impact on viability < 50 μM; Table 1). Both compounds activated the eukaryotic initiation factor 2 (ElF2) signalling pathway, the eukaryotic integrated stress response (ISR) and the resulting signaling network, together with autophagy and sirtuin-1 signaling pathways (Fig. 11). Their results suggested that the compounds triggered an innate antiviral response. Previous studies have shown that narciclasine and other alkaloids interact with larger ribosome subunits, inhibiting peptide bond formation, with eukaryotic translation elongation factor 1A necessary for elongating ribosomes, and inhibiting Hsp70, which affects a broad range of viruses.[125,126] The authors further tested the dihydronarciclasine analog *in vivo* and reported a delayed and decreased viral titer in a mouse model of HSV-1 ocular infection.

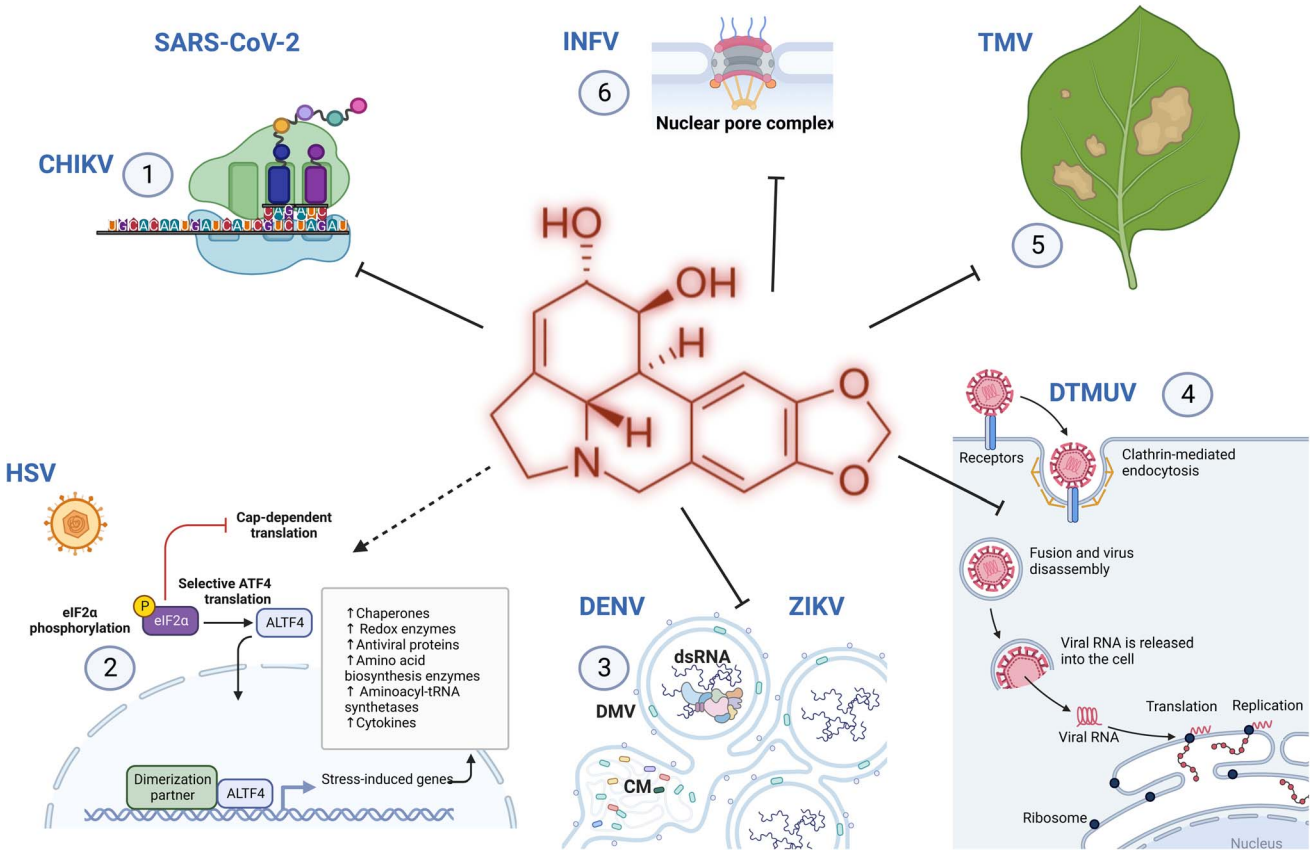

Fig. 11 Multiple targets of antiviral Amaryllidaceae alkaloids. AAs such as lycorine target ribosomal translation during infection with chikungunya virus (CHIKV) and SARS-CoV-2 (1), trigger stress-induced and innate responses to counter herpes simplex virus (HSV) replication (2), target the RNA synthesis step of flaviviruses, such as Zika virus (ZIKV) and dengue virus (DENV) (3), inhibit Duck Tembusu Virus (DTMUV) at a post-entry step (4), decrease leaves damages caused by Tobacco Mosaic Virus (TMV) infection, triggering defense enzyme activity (5), and traps the influenza virus (INFV) at the nuclear pore complex (6). Created using Biorender.

3.8 Tobacco mosaic virus

Viruses target all living forms, such as the tobacco mosaic virus (TMV) from the genus *Tobamovirus*, which infects a wide range of plants, damaging crops of tobacco, all Solanaceae family members, ornamental plants, cucumbers, and beans. Hu *et al.* investigated the ethanolic extract of *Lycoris aurea* bulbs and their alkaloids for their anti-TMV activity.[127] Lycorine and some derivatives display protective effects (15.3 and 45.2%) at high concentrations of 100 and 500 mg L^{-1} (0.348 mM and 1.74 mM) in contrast with galanthamine and lycoramine, which did not display any antiviral activity at 100 mg L^{-1}. Yang *et al.* tested AA isolated from the bulbs of *L. radiata*, including sanguinine, 11-hydroxyvittatine, lycoramine, pancratinine C, homolycorine, hippeastrine, *O*-demethylhomolycorine *N*-oxide, zephyranthine, *O*-methyllycorenine *N*-oxide, lycoranine C, tazettine, lycorine, 9-*O*-demethylhomolycorine, homolycorine *N*-oxide, galanthamine, and lycoricidine derivatives owing to their anti-TMV properties *in vivo* by the conventional half-leaf method and on systemic infection by western blot and RT-PCR analysis.[128] Some compounds, such as 11-hydroxyvittatine, zephyranthrine, and lycoranine C, displayed a moderate protective effect. Lycoricidine derivatives showed significant antiviral effects, particularly L1 (*N*-methyl-2,3,4-trimethoxylycoricidine) (60.8% of protective inhibitory activity at 100 μg mL^{-1}) and L3 (*N*-methyl-2-methoxy-3,4-acetonidelycoricidine) (62.0%), which were almost similar to the positive control, ningnanmycin (66.4%). L1, L3, and L5 (*N*-allyl-2,3,4-triallyloxylycoricidine) antiviral activity was further evidenced by a reduction in TMV-coat protein expression. Finally, the authors showed that L1 also triggered defensive enzyme activities (phenylalanine ammonia lyase, peroxidase and superoxide dismutase) in systemic leaves, which is a strategy that could be used to improve disease resistance to tobacco (Fig. 11). These studies pave the way for the possible role of AAs as antiviral compounds in fighting plant diseases.

4 Structure activity relationship

4.1 SARS-CoV-2 and lycorine

4.1.1 RNA replication and transcription. RNA viral RNA replication and transcription require a virus-encoded RdRp, an enzyme that is absent from the infected cell proteome. This makes RdRp an attractive anti-viral drug target. Docking analysis by Jin *et al.* in 2020 suggested that lycorine targets coronavirus RNA replication through interaction with RdRp, hydrogen bonding of C9 methylenedioxy oxygen and the C2 hydroxyl group with Asp263, and catalytic subunit active site residues Asn691 and Ser759.[6] On the other hand, Ren *et al.* proposed that the

amine and aromatic groups of lycorine, present in other known antivirals, such as chloroquine and emetine, are key pharmacophores of RdRp inhibitors.[2] They further showed that the lycorine inhibition of RdRp depends on the presence of RNA at the RNA growth site of nsp12 RdRp using surface plasmon resonance (SPR) and docking, as mentioned in Subsection 3.1.

4.1.2 Translation and polyprotein processing. The genome of coronaviruses and other RNA viruses, such as flaviviruses or alphaviruses, encodes a polyprotein translated by the cellular machinery and is further processed by viral and cellular-encoded proteases. Jin *et al.* suggested that lycorine C1 and C2 hydroxyl and amine pharmacophores are also involved in lycorine interactions with the programmed ribosomal frameshifting element of the SARS-CoV-2 genome, an RNA secondary structure at the junction between open reading frame 1 a (orf1a) and orf1b, critical for proper stoichiometry of non-structural proteins, and hence for the viral life cycle.[2,129] They detected a salt–bridge interaction between the lycorine amine group and the phosphodiester linkage of U13, as well as a hydrogen bond network between the two hydroxyl groups and ribonucleotides. They further predicted that these hydroxyl groups are important for the inhibition of translation through interactions with the ribosome peptidyl transfer site and are stabilized by the hydrogen bonds formed with A4397, U4450, U4446, and G4393. In addition to these interactions, a coordinated bond was observed between the hydroxyl group at C2 and Mg^{2+}.[2] Another study also detected a critical role of these same pharmacophores in SARS-CoV-2 main protease inhibition (Fig. 12). Lycorine partially occupied the enzyme active site, forming H-bonds with Gln189, Glu166, and Asn142 through its nitrogen, impairing correct polyprotein processing.[4]

4.1.3 Assembly. In addition to the apparent key role of these groups in viral inhibition, C10 methylenedioxy oxygen and the adjacent ring A have been implicated in interactions

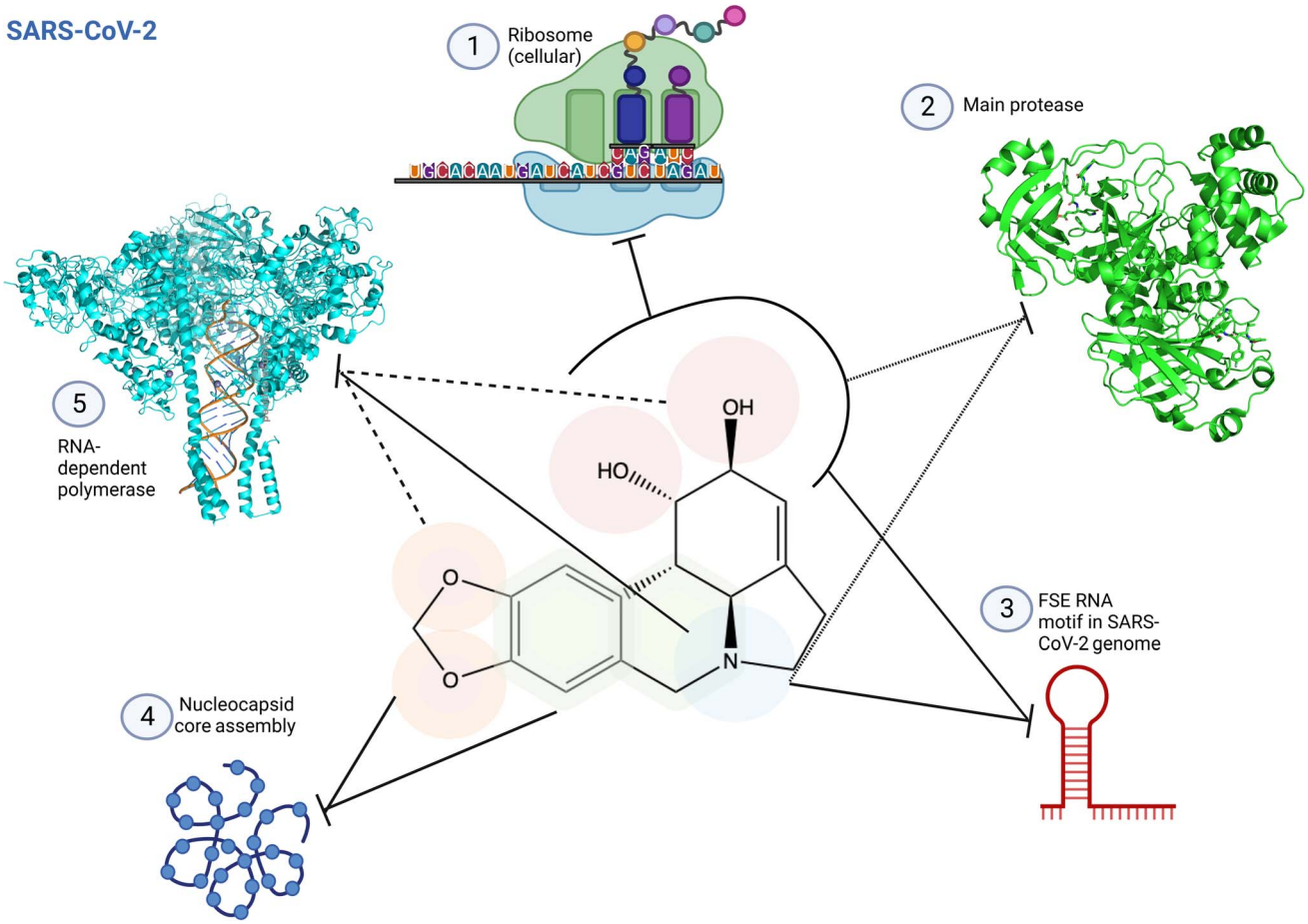

Fig. 12 Structure activity relationship of lycorine specific to SARS-CoV-2. (1) Lycorine C1 and C2 hydroxyl groups are predicted to interact with the ribosome peptidyl transfer site, inhibiting protein translation.[2] (2) C1 and C2 hydroxyl groups and the amine base are predicted to be involved in SARS-CoV-2 main protease inhibition occupying partially the enzyme active site (PDB: 7P35). This impaired correct polyprotein processing.[4] (3) These pharmacophores are also involved in the interactions with the frameshifting element of SARS-CoV-2 genome, preventing correct translation.[2] (4) Lycorine oxygens on methylenedioxy C8 and C9, and interactions with the adjacent ring prevent virus maturation, targeting nucleocapsid core assembly through π-stacking and hydrogen bonding.[2] (5) Lycorine blocks coronavirus RNA replication through C1 and C2 hydroxyl groups, and C9 oxygen[6] and/or through its amine-containing ring[2] by interacting with RNA in the RNA-dependent RNA polymerase (RdRp) active site, as predicted by docking, surface plasma resonance (SPR) and structure similarity with known inhibitor (PDB: 8GWG). Small dashed lines reference to[4] using antiviral assays and docking; full dash lines reference to[6] using cell protease assay, *in cellulo* antiviral assays and docking; and full lines reference to[2] using docking, SPR and antiviral *in cellulo* assays as main methods. Created using Biorender.

with a coronavirus structural protein. *In silico* prediction suggests that lycorine impairs virus maturation by targeting the structural nucleocapsid core assembly through hydrogen bonding and π-stacking with these pharmacophores to prevent virus maturation.[2]

4.1.4 Unidentified targets. Strikingly, 2-*epi*-lycorine, which differs only by one stereocenter at C2, did not display anti-coronaviral and cytotoxic properties,[109] suggesting that ring C plays an important role in ligand–host interaction and that the chirality of C-2 is key to improving potency and removing cytotoxicity, at least in the Vero-E6 cell line.

4.1.5 General conclusion on lycorine anti-coronaviral activity. Although most methods employed in the publications analyzed here are robust, some rely mostly on computational predictions and on *in vitro* (protein-compound interaction and affinity) data. The weight of each interaction *in cellullo* and *in vivo* on viral replication, *i.e.* the relative relevance of lycorine inhibition of correct viral polyprotein translation or nucleocapsid assembly on viral inhibition, has not been measured directly, which will be crucial to verify the importance of each pharmacophore.

4.2 Herpes-simplex virus

4.2.1 Narciclasine and lycoricidine derivatives targeting host factors. In 2018, Brown *et al.* developed 10*b*-aza-analogues of *trans*-hydronarciclasine and *trans*-hydrolycoricidine with ring fusion-modified derivatives, which completely lost their anti-

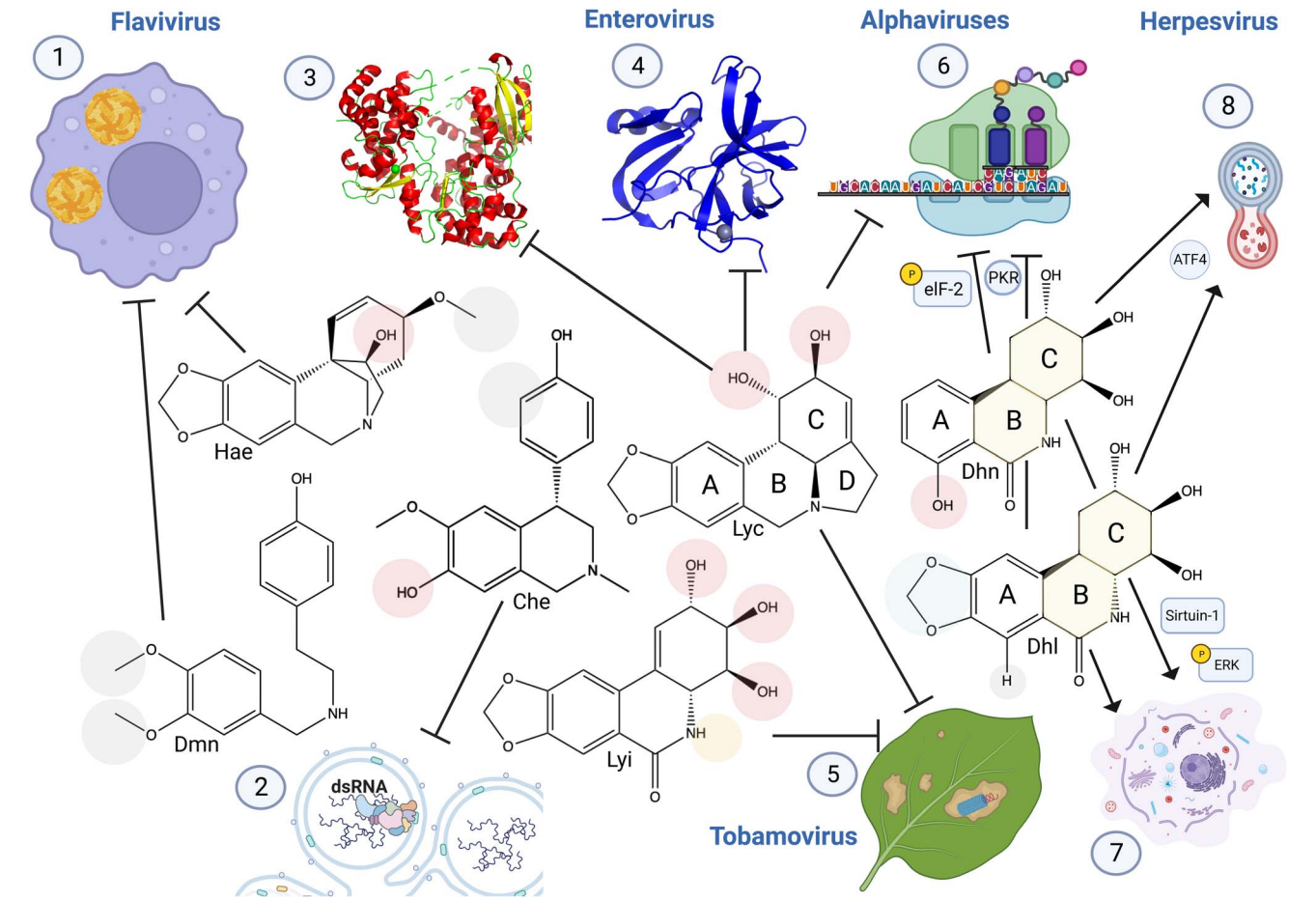

Fig. 13 Structure activity relationship of anti-viral Amaryllidaceae alkaloids. (1) Haemanthamine structural conformation of C11 hydroxyl and C3 methoxy groups are required for DENV inhibition.[1] 3′,4′-*O*-Dimethylnorbelladine methyl groups increased anti-DENV activity.[3] (2) Cherylline non-methylated 3′OH (compared to gigantelline), and the absence of hydroxyl group on the phenol cycle C3 (compared to gigantellinine) is required for its anti-viral activity specific to RNA replication (PDB: 5WZ3).[5] (3) Lycorine C1 hydroxyl group interacts with Zika virus RNA-dependent RNA polymerase to block RNA synthesis, (as shown by *in vitro* enzyme assay, docking evidence, and interaction with His110). (4) Addition of a functional group on this hydroxyl conserves lycorine inhibition of enteroviruses 2A proteinase with reduced cytotoxicity (higher selectivity index), resulting also in a loss of RNA replication (PDB: 3W95).[7,8] (5) Lycorine and lycoricidine derivatives block Tobacco Mosaic Virus. Modifications of lycorine C1 and C2 and of lycoricidine ring C and B functional groups modulate anti-TMV activity. (6) Lycorine C1 and C2 are required to block alphavirus replication through viral RNA translation inhibition.[9] 7-Hydroxyl derivative *trans*-dihydrolycoricidine, and dihydronarciclasine analog with ring-A mono-substituted and C7-OH with fully functionalized ring-C targets herpesvirus replication,[13] affecting eukaryotic initiation factor 2 (eIF2) pathway involved in protein translation.[14] (7) These derivatives also triggered autophagy and (8), apoptosis-related signaling pathways involving ERK and Sirtuin-1. Hae: haemanthamine, Dmn, 3′4′-*O*-dimethylnorbelladine, Che: cherylline, Lyc: lycorine, Lyi: lycoricidine: Dhn: a dihydronarciclasine analog with ring-A mono-substituted and C7-OH, Dhl: *trans*-dihydrolycoricidine. Created using Biorender.

HSV activity, showing that π-type secondary orbital interactions with rings B and C may be critical for their properties.[13] Pioneer studies have shown that the conformational arrangement of narciclasine's C-ring is critical for its protein synthesis inhibitor properties and that the acetylation of its hydroxyl compromised its activity.[125,130] 7-Hydroxyl derivative *trans*-dihydrolycoricidine and dihydronarciclasine analog lacking the methylenedioxy group, with a C7-OH on ring-A, and a fully functionalized ring-C (no double bond but 3 hydroxyl in a similar orientation as lycoricidine) efficiently targeted HSV replication, whereas other modifications of dihydronarciclasine analog, including hydroxylation or *O*-methylation of C9, were not active.[13] As both derivatives affected the elF2 pathway involved in protein translation,[14] triggered autophagy and apoptosis-related signalling pathways involving ERK and Sirtuin-1, ring B and C stereocenters appear to be key to their activity. Previous studies by Gabrielsen and Jimenez *et al.* showed that ring C hydroxyls were crucial for antiviral activity and that the C1–C10b double bond was associated with increased cytotoxicity, while C7 deoxy derivatives led to lower cytotoxic properties.[104,125] The hydroxyl group on C7 was also specifically associated with flaviviral inhibition.

4.3 Zika and dengue virus

4.3.1 Cherylline key pharmacophores to block RNA synthesis. Docking analysis suggested that lycorine C1 hydroxyl interacted with ZIKV RdRp His110 residue to block RNA synthesis.[111] Cherylline non-methylated 3′OH and the absence of a hydroxyl group on the phenol cycle C3 are required for its anti-viral activity specific to RNA replication, as shown by the loss of activity of gigantelline and gigantellinine, respectively.[5]

4.3.2 New antiviral activities and known host targets. Although lycorine's basic N5 and the C3–C4 double bond have to be preserved for its activity, acylation of C1 hydroxyl and oxidation of C2 hydroxyl were previously shown to slightly increase its anti-flaviviral activity but decrease its cytotoxicity.[131] Alternatively, the lycorine specificity of the Wnt/β-catenin pathway, which is associated with its anti-HCV and -enterovirus activity, was shown to require a methyl group at C4 and basic nitrogen at N5, and the addition of a lipophilic group, pyrazole and pyridine at C8 or C9 oxygens increased its activity.[132]

Haemanthamine specific conformational structure of C11 hydroxyl, C3 methoxy groups and ring C1–C10b and C1–C2 bonds are key to its DENV inhibition, as suggested by comparison with 11-hydroxyvittatine and with other very similar compounds being less active.[1] Previous studies had shown that haemanthamine binding to the 25S rRNA A-site cleft induced a 'flip up' conformation of residue U2875, which was not observed upon narciclasine binding and was attributed to the absence of the phenolic hydroxyl in haemanthamine.[113] In addition, haemanthamine interacted with rRNA, whereas narciclasine did not. A haemanthamine aromatic ring fused to the methylenedioxy moiety could form π-stacking interactions with the nucleotide base residues U2875 and C2821 sandwiching the AA. Haemanthamine amino group further reinforced interaction with U2875 through hydrogen bonding, stabilizing the 'flip-up' conformation of the uracil residue. Its C11-hydroxyl group on the ethanol bridge was implicated in two additional H-bonds with U2873. *O*-Acylation of C11 resulted in compromised activity, and the α-configured ethanol bridge was required for rRNA binding. Interestingly, these pharmacophores have been implicated in antiviral activities in previous studies (Fig. 13).[133]

In less studied ring types, 3′,4′-*O*-dimethylnorbelladine methyl groups increased anti-DENV activity compared to single-methylated *O*-norbelladine, suggesting a key role played by these two functional groups in its interaction with its target although not yet characterized.[3] In contrast, norcraugsodine *O*-methylation abolished its anti-DENV potential and reduced its cytotoxicity, indicating the structure–activity relationship of norbelladine-type alkaloids.

4.4 Enterovirus, alphavirus and tobamovirus

Similar to flavivirus-related SAR, the addition of more complex functional groups to lycorine C1 conserved lycorine inhibition of enteroviruses 2A proteinase with reduced cytotoxicity, resulting in a loss of RNA replication.[7,8] Likewise, acetylation, methylation or replacement with Cl of lycorine C1 or C2 hydroxyl and of lycoricidine C2, C3, C4 and N increased anti-TMV properties. In contrast, lycorine C1 and C2 hydroxyl groups are required for blocking alphavirus CHIKV replication through viral RNA translation inhibition,[9] and acetylation at these positions results in a loss of activity.

4.5 Current challenges in the AA structure–activity relationship

Although recent studies confirm and unravel key pharmacophores, the analysis also shows that modifications can yield a virus-specific impact. AAs inhibit multiple viruses and may interact with diverse targets. This complicates the analysis of the relative importance of each functional group to each of its biological properties. Future studies will need to combine powerful systematic biological methods and thorough structure–activity relationship analysis to gather key knowledge to fight viral diseases while preserving cellular processes, such as protein synthesis, proliferation and stress response, but also assessing solvability and brain blood barrier permeability.[134] Moreover, AA pleiotropy might be their greatest strength because it multiplies the mechanisms required for virus escape.

5 Conclusions

Recent studies have highlighted the potential of AA as a scaffold for developing new antiviral compounds for both humans and plants. In recent years, lycorine has been predominantly studied probably owing to its potency, its broad spectrum of targeted microorganisms and its relative abundance in many plants. Lycorine is also readily commercially available. However, some of its biological characteristics prevent its safe use in humans: its broad spectrum implies that it may alter non-desired cellular targets, leading to additional undesired side effects. Lycorine is

cytotoxic to many human cells at low concentrations, and it is highly poisonous to humans when ingested, leading to diarrhea, vomiting, convulsions and even deaths (http://www.t3db.ca/toxins/T3D4064). Consequently, research should continue to focus on structure–activity relationships with the help of computational analysis. Finally, the discovery of the full antiviral spectrum of the other ~650 AA should be encouraged.

Natural product chemists, synthetic organic chemists, biochemists, and bioengineers have co-contributed to the research interest and understanding enrichment of Amaryllidaceae alkaloid structural diversity. All these fronts examine the interpretation and execution of AA for the benefit of mankind. Although it is dubious which method is most appropriate for the sustainable supplementation of AA in the pharmaceutical and medicinal sectors in the long run, AA structural diversity could serve as antiviral components, as emphasized in this review. Further, an improved understanding of biosynthetic pathways could support overcoming the limitations of synthetic biological approaches. However, these are achievable through interdisciplinary research in the aforementioned fields. Thus, this article serves as a tool to facilitate our objectives.

6 Author contributions

Thilina U. Jayawardena and Natacha Merindol: conceptualization, methodology, writing original draft, writing, reviewing, and editing; Nuwan Sameera Liyanage: conceptualization, methodology, writing, reviewing, and editing; Isabel Desgagné-Penix: resources, funding acquisition, supervision, writing – reviewing and editing.

7 Conflicts of interest

There are no conflicts to declare.

8 Acknowledgements

This research was funded by the Canada by the Natural Sciences and Engineering Research Council of Canada (NSERC) award number RGPIN-2021-03218 and the Canada Research Chair on plant specialized metabolism Award No. 950-232164. Many thanks are extended to the Canadian taxpayers and to the Canadian government for supporting the Canada Research Chairs Program.

9 References

1 M. Masi, R. Di Lecce, N. Merindol, M. P. Girard, L. Berthoux, I. Desgagne-Penix, V. Calabro and A. Evidente, *Toxins*, 2022, **14**, 262.
2 P. X. Ren, W. J. Shang, W. C. Yin, H. Ge, L. Wang, X. L. Zhang, B. Q. Li, H. L. Li, Y. C. Xu, E. H. Xu, H. L. Jiang, L. L. Zhu, L. K. Zhang and F. Bai, *Acta Pharmacol. Sin.*, 2022, **43**, 483–493.
3 M. P. Girard, V. Karimzadegan, M. Heneault, F. Cloutier, G. Berube, L. Berthoux, N. Merindol and I. Desgagne-Penix, *Molecules*, 2022, **27**, 5621.
4 A. Narayanan, M. Narwal, S. A. Majowicz, C. Varricchio, S. A. Toner, C. Ballatore, A. Brancale, K. S. Murakami and J. Jose, *Commun. Biol.*, 2022, **5**, 169.
5 S. Ka, N. Merindol, I. Seck, S. Ricard, A. Diop, C. S. B. Boye, K. Landelouci, B. Daoust, L. Berthoux, G. Pepin, M. Seck and I. Desgagne-Penix, *Molecules*, 2021, **26**, 7382.
6 Y. H. Jin, J. S. Min, S. Jeon, J. Lee, S. Kim, T. Park, D. Park, M. S. Jang, C. M. Park, J. H. Song, H. R. Kim and S. Kwon, *Phytomedicine*, 2021, **86**, 153440.
7 H. Wang, T. Guo, Y. Yang, L. Yu, X. Pan and Y. Li, *Front. Cell. Infect. Microbiol.*, 2019, **9**, 277.
8 Y. Guo, Y. Wang, L. Cao, P. Wang, J. Qing, Q. Zheng, L. Shang, Z. Yin and Y. Sun, *Antimicrob. Agents Chemother.*, 2016, **60**, 913–924.
9 N. Li, Z. Wang, R. Wang, Z. R. Zhang, Y. N. Zhang, C. L. Deng, B. Zhang, L. Q. Shang and H. Q. Ye, *Virol. Sin.*, 2021, **36**, 1465–1474.
10 V. M. Dembitsky, *Bioorg. Khim.*, 2002, **28**, 196–208.
11 K. C. Guven, A. Percot and E. Sezik, *Mar. Drugs*, 2010, **8**, 269–284.
12 J. C. Braekman, D. Daloze and J. M. Pasteels, in *Alkaloids*, ed. M. F. Roberts and M. Wink, Springer US, Boston, MA, 1998, ch. 15, pp. 349–378.
13 C. E. Brown, T. Kong, J. F. Britten, N. H. Werstiuk, J. McNulty, L. D'Aiuto, M. Demers and V. L. Nimgaonkar, *ACS Omega*, 2018, **3**, 11469–11476.
14 J. McNulty, C. Babu-Dokuburra, J. Scattolon, C. Zepeda-Velazquez, M. A. Wesesky, J. K. Caldwell, W. Zheng, J. Milosevic, P. R. Kinchington, D. C. Bloom, V. L. Nimgaonkar and L. D'Aiuto, *Sci. Rep.*, 2023, **13**, 1639.
15 P. Dey, A. Kundu, A. Kumar, M. Gupta, B. M. Lee, T. Bhakta, S. Dash and H. S. Kim, in *Recent Advances in Natural Products Analysis*, ed. A. Sanches Silva, S. F. Nabavi, M. Saeedi and S. M. Nabavi, Elsevier, 2020, pp. 505–567.
16 R. Verpoorte, in *Encyclopedia of Analytical Science*, ed. P. Worsfold, A. Townshend and C. Poole, Elsevier, Oxford, 2005, pp. 56–61.
17 G. A. Beaudoin and P. J. Facchini, *Planta*, 2014, **240**, 19–32.
18 R. Verpoorte, in *Encyclopedia of Separation Science*, ed. I. D. Wilson, Academic Press, Oxford, 2000, pp. 1949–1956.
19 T. A. P. Group, *Bot. J. Linn. Soc.*, 2003, **141**, 399–436.
20 M. J. M. Christenhusz and J. W. Byng, *Phytotaxa*, 2016, **261**, 201–217.
21 J. C. Cedrón, M. Del Arco-Aguilar, A. Estévez-Braun and Á. G. Ravelo, in *The Alkaloids: Chemistry and Biology*, ed. G. A. Cordell, Academic Press, 2010, vol. 68, pp. 1–37.
22 A. W. Meerow, J. Francisco-Ortega, D. N. Kuhn and R. J. Schnell, *Syst. Bot.*, 2006, **31**, 42–60.
23 I. Desgagné-Penix, *Phytochem. Rev.*, 2020, **20**, 409–431.
24 S. Ka, M. Koirala, N. Merindol and I. Desgagne-Penix, *Molecules*, 2020, **25**, 4901.
25 J. J. Nair and J. Van Staden, *J. Ethnopharmacol.*, 2014, **151**, 12–26.

26 J. J. Nair, A. Wilhelm, S. L. Bonnet and J. van Staden, *Bioorg. Med. Chem. Lett.*, 2017, **27**, 4943–4951.
27 D. K. Liscombe, B. P. Macleod, N. Loukanina, O. I. Nandi and P. J. Facchini, *Phytochemistry*, 2005, **66**, 1374–1393.
28 T. Ahmed, A. U. Gilani, M. Abdollahi, M. Daglia, S. F. Nabavi and S. M. Nabavi, *Pharmacol. Rep.*, 2015, **67**, 970–979.
29 E. Plazas, S. Hagenow, M. Avila Murillo, H. Stark and L. E. Cuca, *Bioorg. Chem.*, 2020, **98**, 103722.
30 J. D. Phillipson, M. F. Roberts and M. Zenk, *The Chemistry and Biology of Isoquinoline Alkaloids*, Springer Science & Business Media, 1985.
31 N. Samanani and P. J. Facchini, *J. Biol. Chem.*, 2002, **277**, 33878–33883.
32 A. Kornienko and A. Evidente, *Chem. Rev.*, 2008, **108**, 1982–2014.
33 M. He, C. Qu, O. Gao, X. Hu and X. Hong, *RSC Adv.*, 2015, **5**, 16562–16574.
34 A. R. Battersby, H. M. Fales and W. C. Wildman, *J. Am. Chem. Soc.*, 2002, **83**, 4098–4099.
35 H. G. Boit, *Chem. Ber.*, 2006, **87**, 1704–1707.
36 A. Brossi, G. Grethe, S. Teitel, W. C. Wildman and D. T. Bailey, *J. Org. Chem.*, 2002, **35**, 1100–1104.
37 A. Brossi and S. Teitel, *J. Org. Chem.*, 2002, **35**, 3559–3561.
38 A. Brossi and S. Teitel, *Tetrahedron Lett.*, 1970, **11**, 417–419.
39 M. A. Schwartz and S. W. Scott, *J. Org. Chem.*, 2002, **36**, 1827–1829.
40 H. Shi, C. Du, X. Zhang, F. Xie, X. Wang, S. Cui, X. Peng, M. Cheng, B. Lin and Y. Liu, *J. Org. Chem.*, 2018, **83**, 1312–1319.
41 H. Yu, R. Lee, H. Kim and D. Lee, *J. Org. Chem.*, 2019, **84**, 3566–3578.
42 S. Ka, M. Masi, N. Merindol, R. Di Lecce, M. B. Plourde, M. Seck, M. Gorecki, G. Pescitelli, I. Desgagne-Penix and A. Evidente, *Phytochemistry*, 2020, **175**, 112390.
43 J. J. Nair, A. L. Andresen, H. B. Papenfus, D. Staerk and J. van Staden, *S. Afr. J. Bot.*, 2020, **131**, 351–359.
44 B. B. Majhi, S. E. Gelinas, N. Merindol, S. Ricard and I. Desgagne-Penix, *Front. Plant Sci.*, 2023, **14**, 1231809.
45 J. R. Lewis, in *Second Supplements to the 2nd Edition of Rodd's Chemistry of Carbon Compounds*, ed. M. Sainsbury, Elsevier, 1991, pp. 165–249.
46 S. Ghosal, A. Shanthy and S. K. Singh, *Phytochemistry*, 1988, **27**, 1849–1852.
47 M. B. Kilgore, C. K. Holland, J. M. Jez and T. M. Kutchan, *J. Biol. Chem.*, 2016, **291**, 16740–16752.
48 A. Singh, M. A. Massicotte, A. Garand, L. Tousignant, V. Ouellette, G. Berube and I. Desgagne-Penix, *BMC Plant Biol.*, 2018, **18**, 338.
49 N. Samanani, D. K. Liscombe and P. J. Facchini, *Plant J.*, 2004, **40**, 302–313.
50 N. Samanani, S. U. Park and P. J. Facchini, *Plant Cell*, 2005, **17**, 915–926.
51 M. B. Kilgore, M. M. Augustin, C. M. Starks, M. O'Neil-Johnson, G. D. May, J. A. Crow and T. M. Kutchan, *PLoS One*, 2014, **9**, e103223.
52 L. Tousignant, A. M. Diaz-Garza, B. B. Majhi, S. E. Gelinas, A. Singh and I. Desgagne-Penix, *Planta*, 2022, **255**, 30.
53 B. Sun, P. Wang, R. Wang, Y. Li and S. Xu, *Int. J. Mol. Sci.*, 2018, **19**, 1911.
54 W. Li, C. Qiao, J. Pang, G. Zhang and Y. Luo, *Int. J. Biol. Macromol.*, 2019, **141**, 680–692.
55 Q. Li, J. Xu, L. Yang, X. Zhou, Y. Cai and Y. Zhang, *Front. Plant Sci.*, 2020, **11**, 519752.
56 Q. Li, J. Xu, Y. Zheng, Y. Zhang and Y. Cai, *Front. Plant Sci.*, 2021, **12**, 713795.
57 F. Aleya, C. Xianmin, H. Anthony and J. Meriel, *Gene*, 2021, **774**, 145424.
58 S. Ghosal, K. S. Saini and S. Razdan, *Phytochemistry*, 1985, **24**, 2141–2156.
59 A. Gesell, M. Rolf, J. Ziegler, M. L. Diaz Chavez, F. C. Huang and T. M. Kutchan, *J. Biol. Chem.*, 2009, **284**, 24432–24442.
60 D. R. Nelson, R. Ming, M. Alam and M. A. Schuler, *Trop. Plant Biol.*, 2008, **1**, 216–235.
61 M. Mizutani and F. Sato, *Arch. Biochem. Biophys.*, 2011, **507**, 194–203.
62 N. Ikezawa, K. Iwasa and F. Sato, *J. Biol. Chem.*, 2008, **283**, 8810–8821.
63 P. Belin, M. H. Le Du, A. Fielding, O. Lequin, M. Jacquet, J. B. Charbonnier, A. Lecoq, R. Thai, M. Courcon, C. Masson, C. Dugave, R. Genet, J. L. Pernodet and M. Gondry, *Proc. Natl. Acad. Sci. U. S. A.*, 2009, **106**, 7426–7431.
64 D. H. R. Barton and T. Cohen, Some biogenetic aspects of phenol oxidation, *Festschrift Prof. Dr. Arthur Stoll*, Birkhäuser, Basel, 1957.
65 J. Eichhorn, T. Takada, Y. Kita and M. H. Zenk, *Phytochemistry*, 1998, **49**, 1037–1047.
66 W. R. Bowman, I. T. Bruce and G. W. Kirby, *J. Chem. Soc. D*, 1969, 1075b–1077b.
67 C. Fuganti and M. Mazza, *J. Chem. Soc. D*, 1971, 1196–1197.
68 C. Fuganti and M. Mazza, *J. Chem. Soc., Perkin Trans. 1*, 1973, 954–956.
69 D. H. R. Barton, G. W. Kirby, J. B. Taylor and G. M. Thomas, *J. Chem. Soc.*, 1963, 4545–4558.
70 M. B. Kilgore, M. M. Augustin, G. D. May, J. A. Crow and T. M. Kutchan, *Front. Plant Sci.*, 2016, **7**, 225.
71 S. Uyeo and S. Kobayashi, *Pharm. Bull.*, 1953, **1**, 139–142.
72 N. Hazama, H. Irie, T. Mizutani, T. Shingu, M. Takada, S. Uyeo and A. Yoshitake, *J. Chem. Soc.*, 1968, 2947–2953.
73 J. Q. Chen, J. H. Xie, D. H. Bao, S. Liu and Q. L. Zhou, *Org. Lett.*, 2012, **14**, 2714–2717.
74 L. Li, Q. Yang, Y. Wang and Y. Jia, *Angew Chem. Int. Ed. Engl.*, 2015, **54**, 6255–6259.
75 S. Majumder, A. Yadav, S. Pal, A. Khatua and A. Bisai, *J. Org. Chem.*, 2022, **87**, 7786–7797.
76 I. T. Bruce and G. W. Kirby, *Chem. Commun.*, 1968, 207–208.
77 C. Fuganti and M. Mazza, *J. Chem. Soc. Chem. Commun.*, 1972, 936–937.
78 W. C. Wildman and N. E. Heimer, *J. Am. Chem. Soc.*, 1967, **89**, 5265–5269.
79 G. W. Kirby and H. P. Tiwari, *J. Chem. Soc. C*, 1966, 676–682.
80 A. R. Battersby, R. Blinks, S. W. Breuer, H. M. Fales, W. C. Wildman and R. J. Highet, *J. Chem. Soc.*, 1964, 1595–1609.

81 R. D. Harken, C. P. Christensen and W. C. Wildman, *J. Org. Chem.*, 2002, **41**, 2450–2454.
82 M. Kihara, L. Xu, K. Konishi, K. Kida, Y. Nagao, S. Kobayashi and T. Shingu, *Chem. Pharm. Bull.*, 1994, **42**, 289–292.
83 M. Kihara, L. XU, K. Konishi, Y. Nagao, S. Kobayashi and T. J. H. Shingu, *Heterocycles*, 1992, **34**, 1299–1301.
84 Y. Nakagawa, S. Uyeo and H. J. C. Yajima, *Chem. Ind.*, 1956, 1238–1239.
85 K. Kotera, Y. Hamada and R. Mitsui, *Tetrahedron*, 1968, **24**, 2463–2479.
86 C. Fuganti and M. Mazza, *J. Chem. Soc. D*, 1970, 1466.
87 C. Fuganti, J. Staunton and A. R. Battersby, *J. Chem. Soc. D*, 1971, 1154–1155.
88 C. Fuganti, *J. Gazz. Chim. Ital.*, 1973, **103**, 1255–1264.
89 M. B. Kilgore, *The Identification of alkaloid pathway genes from Non-Model Plant Species in the Amaryllidaceae*, Washington University in St. Louis, 2015.
90 C. Fuganti and M. Mazza, *J. Chem. Soc. Chem. Commun.*, 1972, 239.
91 A. I. Feinstein and W. C. Wildman, *J. Org. Chem.*, 2002, **41**, 2447–2450.
92 H. M. Fales and W. C. Wildman, *J. Am. Chem. Soc.*, 2002, **86**, 294–295.
93 W. C. Wildman and D. T. Bailey, *J. Am. Chem. Soc.*, 2002, **89**, 5514–5515.
94 C. Giró Mañas, V. L. Paddock, C. G. Bochet, A. C. Spivey, A. J. White, I. Mann and W. Oppolzer, *J. Am. Chem. Soc.*, 2010, **132**, 5176–5178.
95 W. C. Wildman and D. T. Bailey, *J. Am. Chem. Soc.*, 2002, **91**, 150–157.
96 S. Danishefsky, J. Morris, G. Mullen and R. Gammill, *J. Am. Chem. Soc.*, 2002, **104**, 7591–7599.
97 H. Haning, C. Giro-Manas, V. L. Paddock, C. G. Bochet, A. J. White, G. Bernardinelli, I. Mann, W. Oppolzer and A. C. Spivey, *Org. Biomol. Chem.*, 2011, **9**, 2809–2820.
98 M. Safratova, J. Kroustkova, N. Maafi, D. Suchankova, R. Vrabec, J. Chlebek, J. Kunes, L. Opletal, F. Bucar and L. Cahlikova, *Plants*, 2022, **11**, 3034.
99 C. K. Briggs, P. F. Highet, R. J. Highet and W. C. Wildman, *J. Am. Chem. Soc.*, 2002, **78**, 2899–2904.
100 C. Fuganti, *Tetrahedron Lett.*, 1973, **14**, 1785–1788.
101 T. Robinson, *Science*, 1974, **184**, 430–435.
102 E. Furusawa, S. Furusawa, J. Y. Lee and S. Patanavanich, *Proc. Soc. Exp. Biol. Med.*, 1976, **152**, 186–191.
103 J. Renard-Nozaki, T. Kim, Y. Imakura, M. Kihara and S. Kobayashi, *Res. Virol.*, 1989, **140**, 115–128.
104 B. Gabrielsen, T. P. Monath, J. W. Huggins, D. F. Kefauver, G. R. Pettit, G. Groszek, M. Hollingshead, J. J. Kirsi, W. M. Shannon, E. M. Schubert, *et al.*, *J. Nat. Prod.*, 1992, **55**, 1569–1581.
105 S. Y. Li, C. Chen, H. Q. Zhang, H. Y. Guo, H. Wang, L. Wang, X. Zhang, S. N. Hua, J. Yu, P. G. Xiao, R. S. Li and X. Tan, *Antiviral Res.*, 2005, **67**, 18–23.
106 Y. N. Zhang, Q. Y. Zhang, X. D. Li, J. Xiong, S. Q. Xiao, Z. Wang, Z. R. Zhang, C. L. Deng, X. L. Yang, H. P. Wei, Z. M. Yuan, H. Q. Ye and B. Zhang, *Emerging Microbes Infect.*, 2020, **9**, 1170–1173.
107 K. Zhang, I. N. Zheludev, R. J. Hagey, M. T. Wu, R. Haslecker, Y. J. Hou, R. Kretsch, G. D. Pintilie, R. Rangan, W. Kladwang, S. Li, E. A. Pham, C. Bernardin-Souibgui, R. S. Baric, T. P. Sheahan, D. S. V. D′Souza, J. S. Glenn, W. Chiu and R. Das, *bioRxiv*, 2020, preprint, DOI: 10.1101/2020.07.18.209270.
108 S. Tan, M. G. Banwell, W. C. Ye, P. Lan and L. V. White, *Chem. – Asian J.*, 2022, **17**, e202101215.
109 N. T. Le, S. De Jonghe, K. Erven, T. Vermeyen, A. M. Balde, W. A. Herrebout, J. Neyts, C. Pannecouque, L. Pieters and E. Tuenter, *Molecules*, 2023, **28**, 3222.
110 T. Zhou, L. Tan, G. Y. Cederquist, Y. Fan, B. J. Hartley, S. Mukherjee, M. Tomishima, K. J. Brennand, Q. Zhang, R. E. Schwartz, T. Evans, L. Studer and S. Chen, *Cell Stem Cell*, 2017, **21**, 274–283.
111 H. Chen, Z. Lao, J. Xu, Z. Li, H. Long, D. Li, L. Lin, X. Liu, L. Yu, W. Liu, G. Li and J. Wu, *Virology*, 2020, **546**, 88–97.
112 G. Zou, F. Puig-Basagoiti, B. Zhang, M. Qing, L. Chen, K. W. Pankiewicz, K. Felczak, Z. Yuan and P. Y. Shi, *Virology*, 2009, **384**, 242–252.
113 S. Pellegrino, M. Meyer, C. Zorbas, S. A. Bouchta, K. Saraf, S. C. Pelly, G. Yusupova, A. Evidente, V. Mathieu, A. Kornienko, D. L. J. Lafontaine and M. Yusupov, *Structure*, 2018, **26**, 416–425.
114 E. de Castro Barbosa, T. M. A. Alves, M. Kohlhoff, S. T. G. Jangola, D. E. V. Pires, A. C. C. Figueiredo, E. A. R. Alves, C. E. Calzavara-Silva, M. Sobral, E. G. Kroon, L. H. Rosa, C. L. Zani and J. G. de Oliveira, *Virol. J.*, 2022, **19**, 31.
115 Z. Cao, C. Zhang, Y. Liu, Y. Liu, W. Ye, J. Han, G. Ma, D. Zhang, F. Xu, X. Gao, Y. Tang, S. Shi, C. Wan, C. Zhang, B. He, M. Yang, X. Lu, Y. Huang, Y. Diao, X. Ma and D. Zhang, *Emerging Infect. Dis.*, 2011, **17**, 1873–1875.
116 J. Su, S. Li, X. Hu, X. Yu, Y. Wang, P. Liu, X. Lu, G. Zhang, X. Hu, D. Liu, X. Li, W. Su, H. Lu, N. S. Mok, P. Wang, M. Wang, K. Tian and G. F. Gao, *PLoS One*, 2011, **6**, e18106.
117 Y. Tang, Y. Diao, X. Gao, C. Yu, L. Chen and D. Zhang, *Transboundary Emerging Dis.*, 2012, **59**, 336–343.
118 X. Lv, M. Zhang, S. Yu, C. Zhang, T. Fang, D. Liu, B. Jia, M. Zhu, B. Wang, Q. Wang, Y. Zhu and G. Wang, *Poult. Sci.*, 2021, **100**, 101404.
119 J. He, W. B. Qi, L. Wang, J. Tian, P. R. Jiao, G. Q. Liu, W. C. Ye and M. Liao, *Influenza Other Respir. Viruses*, 2013, **7**, 922–931.
120 L. Yang, J. H. Zhang, X. L. Zhang, G. J. Lao, G. M. Su, L. Wang, Y. L. Li, W. C. Ye and J. He, *PeerJ*, 2019, **7**, e7697.
121 J. He, H. Huang, B. Li, H. Li, Y. Zhao, Y. Li, W. Ye, W. Qi, W. Tang and L. Wang, *Front. Microbiol.*, 2022, **13**, 862205.
122 B. Cox and F. Levent, *JAMA*, 2018, **320**, 2492.
123 J. Liu, Y. Yang, Y. Xu, C. Ma, C. Qin and L. Zhang, *Virol. J.*, 2011, **8**, 483.
124 W. J. van Zuylen, W. D. Rawlinson and C. E. Ford, *Rev. Med. Virol.*, 2016, **26**, 340–355.
125 A. Jimenez, A. Santos, G. Alonso and D. Vazquez, *Biochim. Biophys. Acta*, 1976, **425**, 342–348.

126 G. Van Goietsenoven, V. Mathieu, F. Lefranc, A. Kornienko, A. Evidente and R. Kiss, *Med. Res. Rev.*, 2013, **33**, 439–455.
127 Z. Hu, Z. Wang, Y. Liu and Q. Wang, *Pest Manage. Sci.*, 2018, **74**, 2783–2792.
128 D. Q. Yang, Z. R. Chen, D. Z. Chen, X. J. Hao and S. L. Li, *Nat. Prod. Bioprospect.*, 2018, **8**, 189–197.
129 C. Roman, A. Lewicka, D. Koirala, N. S. Li and J. A. Piccirilli, *ACS Chem. Biol.*, 2021, **16**, 1469–1481.
130 A. Baez and D. Vazquez, *Biochim. Biophys. Acta*, 1978, **518**, 95–103.
131 P. Wang, L. F. Li, Q. Y. Wang, L. Q. Shang, P. Y. Shi and Z. Yin, *ChemMedChem*, 2014, **9**, 1522–1533.
132 D. Z. Chen, C. X. Jing, J. Y. Cai, J. B. Wu, S. Wang, J. L. Yin, X. N. Li, L. Li and X. J. Hao, *J. Nat. Prod.*, 2016, **79**, 180–188.
133 N. Suzuki, S. Tani, S. Furusawa and E. Furusawa, *Proc. Soc. Exp. Biol. Med.*, 1974, **145**, 771–777.
134 E. Kohelova, R. Perinova, N. Maafi, J. Korabecny, D. Hulcova, J. Marikova, T. Kucera, L. Martinez Gonzalez, M. Hrabinova, K. Vorcakova, L. Novakova, A. De Simone, R. Havelek and L. Cahlikova, *Molecules*, 2019, **24**, 1307.